

TWO- AND THREE-POINT FUNCTIONS IN THE EXTENDED NJL MODEL

Johan Bijnens^a and Joaquim Prades^{a,b}

^a NORDITA, Blegdamsvej 17,
DK-2100 Copenhagen Ø, Denmark

^b Niels Bohr Institute, Blegdamsvej 17,
DK-2100 Copenhagen Ø, Denmark

Abstract

The two-point functions in generalized Nambu–Jona-Lasinio models are calculated to all orders in momenta and quark masses to leading order in $1/N_c$. The use of Ward identities and the heat-kernel expansion allows for a large degree of regularization independence. We also show how this approach works to the same order for three-point functions on the example of the vector-pseudoscalar-pseudoscalar three-point function. The inclusion of the chiral anomaly effects at this level is shown by calculating the pseudoscalar-vector-vector three-point function to the same order. Finally we comment on how (vector-)meson-dominance comes out in the presence of explicit chiral symmetry breaking in both the anomalous and the non-anomalous sectors.

March 1994
revised April 1994

1 Introduction

The Extended Nambu–Jona-Lasinio model (ENJL)[1, 2] has already a long history. For some recent reviews see [3] and references therein. Generally a good agreement with low-energy hadronic phenomenology has been found. However its main drawback is the lack of confinement. In ref. [4] a large number of relations between the observables was found which were valid in a large class of ENJL-like models. In ref. [5] this type of relations was generalized to two-point functions and to all orders in the momenta in the chiral limit. Various numerical results obtained in ref. [6] thus obtained a larger range of validity. In this work we shall extend this type of analysis to three-point functions and two-point functions beyond the chiral limit. The first one, the vector-pseudoscalar-pseudoscalar can already be found in [7] and we have included it to show explicitly the use of one-loop Ward identities to simplify the calculation. A similar approach can be found in ref.[8] which we received when the analytic part of this work was essentially finished. They have a less general treatment of regularization dependence than is done here and only treat the case with equal current-quark masses. With the same definitions our results for the two-point functions agree with theirs. Our main aim is to apply this procedure to the case of the pseudoscalar-vector-vector three-point function. Here we both illustrate our prescription for the consistent treatment of the chiral anomaly in this model by imposing the QCD anomalous Ward identities [9]. The latter do imply the use of consistent one-loop ENJL anomalous Ward identities. We find that the duality between the Vector-Meson-Dominance (VMD) picture for the slope of the anomalous $\pi^0\gamma\gamma$ form factor and the quark-loop one is much worse than the one found for the pion electromagnetic form factor and a more refined model (like ENJL cut-off like models) is necessary to reconcile both approaches.

At this point we would like to add some comments about the anomaly in the ENJL model. In [10] it has been argued that the anomaly can not be consistently reproduced in this type of models. While we agree that in general in these models no simple definition of the anomaly is possible, we believe, as discussed in [9], that if one wants to use these models as a low-energy approximation to QCD there is a unique prescription of how to do this. Other uncertainties in the regularization scheme of the anomalous sector will be suppressed by powers of the cut-off Λ_χ used in the ENJL model.

The paper is organized as follows. In section 2 we give a short overview of the ENJL model. Here we also discuss the dependence of the constituent quark mass on the current quark mass and make some remarks about the definition of quarks versus the QCD ones. In section 3 we extend the analysis of ref. [5] to the case with nonzero current quark masses and both masses that play a rôle in the two-point function are allowed to be different. We compare the results with Chiral Perturbation Theory (χ PT) and show numerical results for some of the two-point functions. We also discuss the method used shortly and give the new

identities that the two-point functions at one-loop and the full resummed ones have to satisfy. Their derivation is rather technical and has been given explicitly in appendix B. The main difference with ref. [5] is that now there is also non-trivial mixing in the scalar sector. In subsection 3.8 we discuss in detail the Weinberg Sum Rules (WSR). It is found that here the high energy behaviour of this class of ENJL-like models is too strongly suppressed.

Then we come to the derivation of the three-point functions here in the next section 4. In subsection 4.1 we discuss the vector-pseudoscalar-pseudoscalar three-point function paying attention to the Ward identities in its calculation. In subsection 4.2 we do the same for the pseudoscalar-vector-vector three-point function. Here we explain how one needs to treat the anomalous part of the Ward identities to get a consistent result. Section 5 treats the appearance of Vector Meson Dominance like features of two- and three-point functions in this class of models. We briefly discuss two-point functions and particularly the transverse vector two-point function in the first subsection. Here the origin of the large shift in the slope compared to $M_V^2(0)$ of ref. [4] is explained. In subsection 5.2 we discuss the VMD behaviour of the first three-point function and give a discussion of the KSRF identity [11] in this ENJL model. In the last subsection we treat the vector-pseudoscalar-pseudoscalar three-point function similarly. In section 6 we summarize our results.

The appendices contain the definition of our regularization procedure, the derivation of the Ward identities and explicit expressions for the one-loop functions we need.

2 Short description of the ENJL model and its connection with QCD

The QCD Lagrangian is given by

$$\begin{aligned}\mathcal{L}_{\text{QCD}} &= \mathcal{L}_{\text{QCD}}^0 - \frac{1}{4}G_{\mu\nu}G^{\mu\nu}, \\ \mathcal{L}_{\text{QCD}}^0 &= \bar{q} \{i\gamma^\mu (\partial_\mu - iv_\mu - ia_\mu\gamma_5 - iG_\mu) - (\mathcal{M} + s - ip\gamma_5)\} q.\end{aligned}\tag{2.1}$$

Here summation over colour degrees of freedom is understood and we have used the following short-hand notations: $\bar{q} \equiv (\bar{u}, \bar{d}, \bar{s})$; G_μ is the gluon field in the fundamental $\text{SU}(N_c)$ (N_c =number of colours) representation; $G_{\mu\nu}$ is the gluon field strength tensor in the adjoint $\text{SU}(N_c)$ representation; v_μ , a_μ , s and p are external vector, axial-vector, scalar and pseudoscalar field matrix sources; \mathcal{M} is the quark-mass matrix.

All indications are that in the purely gluonic sector there is a mass-gap. Therefore there seems to be a kind of cut-off mass in the gluon propagator (see the

discussion in ref. [12]). Alternatively one can think of integrating out the high-frequency (higher than Λ_χ , a cut-off of the order of the spontaneous symmetry breaking scale) gluon and quark degrees of freedom and then expand the resulting effective action in terms of local fields. We then stop this expansion after the dimension six terms. This leads to the following effective action at leading order in the $1/N_c$ expansion

$$\begin{aligned}
\mathcal{L}_{\text{QCD}} &\rightarrow \mathcal{L}_{\text{QCD}}^{\Lambda_\chi} + \mathcal{L}_{\text{NJL}}^{\text{S,P}} + \mathcal{L}_{\text{NJL}}^{\text{V,A}} + \mathcal{O}(1/\Lambda_\chi^4), \\
\text{with } \mathcal{L}_{\text{NJL}}^{\text{S,P}} &= \frac{8\pi^2 G_S(\Lambda_\chi)}{N_c \Lambda_\chi^2} \sum_{i,j} (\bar{q}_R^i q_L^j) (\bar{q}_L^j q_R^i) \\
\text{and } \mathcal{L}_{\text{NJL}}^{\text{V,P}} &= -\frac{8\pi^2 G_V(\Lambda_\chi)}{N_c \Lambda_\chi^2} \sum_{i,j} [(\bar{q}_L^i \gamma^\mu q_L^j) (\bar{q}_L^j \gamma_\mu q_L^i) + (L \rightarrow R)].
\end{aligned} \tag{2.2}$$

Where i, j are flavour indices and $\Psi_{R,L} \equiv (1/2)(1 \pm \gamma_5)\Psi$. The couplings G_S and G_V are dimensionless and $\mathcal{O}(1)$ in the $1/N_c$ expansion and summation over colours between brackets is understood. The Lagrangian $\mathcal{L}_{\text{QCD}}^{\Lambda_\chi}$ includes only low-frequency modes of quark and gluon fields. The remaining gluon fields can be assumed to be fully absorbed in the coefficients of the local quark field operators or alternatively also described by vacuum expectation values of gluonic operators (see the discussions in refs. [4, 5]). In the mean-field approximation these $\mathcal{L}_{\text{NJL}}^{\text{S,P,V,A}}$ above are equivalent to a constituent chiral quark-mass term [13].

This model has the same symmetry structure as the QCD action at leading order in $1/N_c$ [14] (notice that the $U(1)_A$ problem is absent at this order [15]). (For explicit symmetry properties under $SU(3)_L \times SU(3)_R$ of the fields in this model see reference [4].) We can self-consistently solve the Schwinger-Dyson equation for the fermion propagator in terms of the bare propagator and a one-loop diagram. In the case where the current quark masses are set to zero this equation allows for two solutions for $G_S > 1$, one with constituent quark mass $M = 0$ and the other with $M \neq 0$ and the model shows spontaneous chiral symmetry breaking. In the presence of explicit chiral symmetry breaking only the second solution is allowed. We shall allow for nonzero current quark masses, $\mathcal{M} = \text{diag}(m_u, m_d, m_s)$ and all different. In the leading $1/N_c$ limit the solution of the Schwinger-Dyson equation is a flavour diagonal matrix for the constituent quark masses with elements $M_{u,d,s}$. The gap-equation now becomes

$$M_i = m_i - g_S \langle 0 | : \bar{q}_i q_i : | 0 \rangle, \tag{2.3}$$

$$\begin{aligned}
\langle 0 | : \bar{q}_i q_i : | 0 \rangle \equiv \langle \bar{q}_i q_i \rangle &= -N_c 4M_i \int \frac{d^4 p}{(2\pi)^4} \frac{i}{p^2 - M_i^2} \\
&= -\frac{N_c}{16\pi^2} 4M_i^3 \Gamma(-1, \epsilon_i),
\end{aligned} \tag{2.4}$$

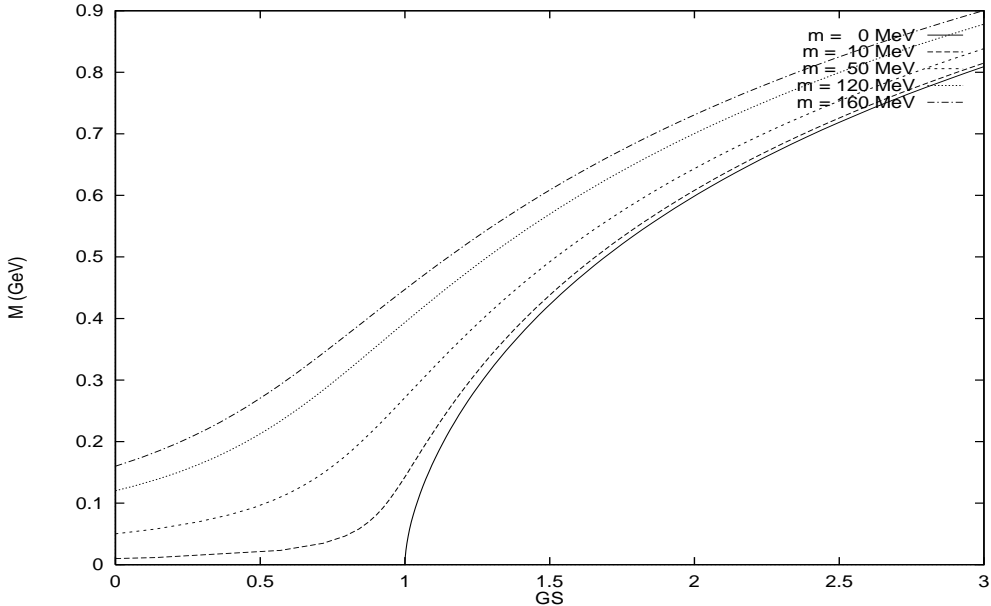


Figure 1: Plot of the dependence of the constituent quark mass M_i as a function of G_S for several values of m_i

$$g_S \equiv \frac{4\pi^2 G_S}{N_c \Lambda_\chi^2} . \quad (2.5)$$

Therefore, in this model the scalar quark-antiquark one-point function (quark condensate) obtains a non-trivial nonzero value. The dependence on the current quark-mass is somewhat obscured in eq. (2.4). We use here a cut-off in proper time as the regulator. See appendix A for its definition. The quantity ϵ_i appearing in (2.4) is M_i^2/Λ_χ^2 . In figure 1 we have plotted the dependence of M_i on G_S for various values of m_i and $\Lambda_\chi = 1.160$ GeV. It can be seen that the value of M_i for small m_i converges smoothly towards the value in the chiral limit for the spontaneously broken phase. This is an indication that an expansion in the quark masses as Chiral Perturbation Theory assumes for QCD is also valid in this model. However, it can also be seen that the validity of this expansion breaks down quickly and for $m_i \simeq 200$ MeV we already have $2M_i \simeq \Lambda_\chi$. We note that the ratio of vacuum expectation values for light quark flavours increases with increasing current quark mass at $p^2 = 0$ in this model and starts to saturate for $m_i > 200$ MeV. In standard χ PT this ratio is taken to be 1 at lowest order and its behaviour with the current quark mass is governed (at $\mathcal{O}(p^4)$) by the following combination of coupling constants $2L_8 + H_2$ [16] in the large N_c limit. The $\mathcal{O}(p^4)$ χ PT coupling constants [16] are calculated at leading order in $1/N_c$ and in the chiral limit in the ENJL model [4]¹. The analytical result for this combination of couplings

¹The analytical expression for H_2 in that reference is correct. The tables contain a numerical error. For example the value of H_2 for the parameters of fit 1 in ref. [4] is $1.4 \cdot 10^{-3}$

constants there was confirmed in ref. [5] from a calculation of the scalar two-point function in the chiral limit and in the large N_c limit to all orders in momenta. This result was obtained by requiring the relevant Ward identities to all orders in momenta. The value for the combination $2L_8 + H_2$ found there corresponds to a big increase of the quark condensate with the current quark mass at this order. We want to emphasize here that the exact identification of the quark condensate in eq. (2.4) which is regularization dependent and especially its dependence on the current quark mass with the one used in χ PT or QCD Sum Rules is by no means straightforward. The differences between both can be traced back in the scalar sector of the model and in particular in the quadratically regularization dependent $\mathcal{O}(p^4)$ coupling constant H_2 [16]. This high-energy constant is related to the details of the integration of the QCD high-frequency modes to obtain the Lagrangian in eq. (2.2). However there are indications that the QCD light quark condensates indeed increase with the current quark mass. In general, there is some uncertainty in the definition of the quark fields in ENJL models versus the QCD ones. This depends on the details on how the ENJL model originates from QCD.

3 Two-point functions in the presence of current quark masses

This section is a generalization of the results in ref. [5] to the case of nonzero current quark masses. These two-point functions were studied before in [6] but there they were discussed as quark form factors. What is new here is that the explicit dependence on the regularization scheme has been put into two arbitrary functions, namely, $\bar{\Pi}_V^{(0)} + \bar{\Pi}_V^{(1)}$ and $\bar{\Pi}_M^P$ (see this section below for definitions). This also shows that these results are valid in a class of models where the one-loop (see further for the definition of this) result can be expanded in a heat-kernel expansion using the same basic quantities E and $R_{\mu\nu}$ as used here. This includes the ENJL model with low-energy gluons described by background expectation values. We have not included this case in our numerical results for the explicit one-loop expressions. For the equal mass case the relevant one loop formulas can be found in ref. [5].

3.1 Definition of the two-point functions

We shall discuss two-point functions of the vector, axial-vector, scalar and pseudoscalar quark currents with the following definitions,

$$V_\mu^{ij}(x) \equiv \bar{q}_i(x)\gamma_\mu q_j(x), \quad (3.1)$$

$$A_\mu^{ij}(x) \equiv \bar{q}_i(x)\gamma_\mu\gamma_5 q_j(x), \quad (3.2)$$

$$S^{ij}(x) \equiv -\bar{q}_i(x)q_j(x), \quad (3.3)$$

$$P^{ij}(x) \equiv \bar{q}_i(x) i\gamma_5 q_j(x), \quad (3.4)$$

The indices i, j are flavour indices and run over u, d, s . The two-point functions themselves are defined as

$$\Pi_{\mu\nu}^V(q)_{ijkl} = i \int d^4x e^{iq \cdot x} \langle 0 | T \left(V_\mu^{ij}(x) V_\nu^{kl}(0) \right) | 0 \rangle, \quad (3.5)$$

$$\Pi_{\mu\nu}^A(q)_{ijkl} = i \int d^4x e^{iq \cdot x} \langle 0 | T \left(A_\mu^{ij}(x) A_\nu^{kl}(0) \right) | 0 \rangle, \quad (3.6)$$

$$\Pi_\mu^S(q)_{ijkl} = i \int d^4x e^{iq \cdot x} \langle 0 | T \left(V_\mu^{ij}(x) S^{kl}(0) \right) | 0 \rangle, \quad (3.7)$$

$$\Pi_\mu^P(q)_{ijkl} = i \int d^4x e^{iq \cdot x} \langle 0 | T \left(A_\mu^{ij}(x) P^{kl}(0) \right) | 0 \rangle, \quad (3.8)$$

$$\Pi^S(q)_{ijkl} = i \int d^4x e^{iq \cdot x} \langle 0 | T \left(S^{ij}(x) S^{kl}(0) \right) | 0 \rangle, \quad (3.9)$$

$$\Pi^P(q)_{ijkl} = i \int d^4x e^{iq \cdot x} \langle 0 | T \left(P^{ij}(x) P^{kl}(0) \right) | 0 \rangle. \quad (3.10)$$

In the leading order in the number of colours these are all proportional to $\delta_{ijkl} \equiv \delta_{il}\delta_{jk}$, with δ_{il} the Kronecker delta. Using Lorentz-invariance these functions can then be expressed as follows

$$\Pi_{\mu\nu}^V(q)_{ijkl} = \left\{ (q_\mu q_\nu - q^2 g_{\mu\nu}) \Pi_V^{(1)}(Q^2)_{ij} + q_\mu q_\nu \Pi_V^{(0)}(Q^2)_{ij} \right\} \delta_{ijkl}, \quad (3.11)$$

$$\Pi_{\mu\nu}^A(q)_{ijkl} = \left\{ (q_\mu q_\nu - q^2 g_{\mu\nu}) \Pi_A^{(1)}(Q^2)_{ij} + q_\mu q_\nu \Pi_A^{(0)}(Q^2)_{ij} \right\} \delta_{ijkl}, \quad (3.12)$$

$$\Pi_\mu^S(q)_{ijkl} = q_\mu \Pi_S^M(Q^2)_{ij} \delta_{ijkl}, \quad (3.13)$$

$$\Pi_\mu^P(q)_{ijkl} = i q_\mu \Pi_P^M(Q^2)_{ij} \delta_{ijkl}, \quad (3.14)$$

$$\Pi^S(q)_{ijkl} = \Pi_S(Q^2)_{ij} \delta_{ijkl}, \quad (3.15)$$

$$\Pi^P(q)_{ijkl} = \Pi_P(Q^2)_{ij} \delta_{ijkl}. \quad (3.16)$$

Here $Q^2 = -q^2$. We shall discuss the Weinberg Sum Rules and numerical results for the two-point functions only in the Euclidean domain, i.e. Q^2 positive. Using Bose symmetry on the definitions of the two-point functions it follows that $\Pi_V^{(0)}(Q^2)_{ij}$, $\Pi_V^{(1)}(Q^2)_{ij}$, $\Pi_A^{(0)}(Q^2)_{ij}$, $\Pi_A^{(1)}(Q^2)_{ij}$, $\Pi_S(Q^2)_{ij}$ and $\Pi_M(Q^2)_{ij}$ are all symmetric in the flavour indices i and j . The remaining ones need the Ward-identities to prove their flavour structure. From the identities in the appendix B it follows that $\Pi_S^M(Q^2)_{ij}$ is also symmetric in i, j ; while $\Pi_P^M(Q^2)_{ij}$ is anti-symmetric.

3.2 Lowest order results in Chiral Perturbation Theory

From Chiral Perturbation Theory to order p^4 in the expansion we obtain the following low energy results for the two-point functions. The orders mentioned behind are the orders in Chiral Perturbation Theory that are neglected.

$$\Pi_V^{(1)}(Q^2)_{ij} = -4(2H_1 + L_{10}) + \mathcal{O}(p^6), \quad (3.17)$$

$$\Pi_V^{(0)}(Q^2)_{ij} = \mathcal{O}(p^6), \quad (3.18)$$

$$\Pi_A^{(1)}(Q^2)_{ij} = \frac{2f_{ij}^2}{Q^2} - 4(2H_1 - L_{10}) + \mathcal{O}(p^6), \quad (3.19)$$

$$\Pi_A^{(0)}(Q^2)_{ij} = 2f_{ij}^2 \left(\frac{1}{m_{ij}^2 + Q^2} - \frac{1}{Q^2} \right) + \mathcal{O}(p^6), \quad (3.20)$$

$$\Pi_S^M(Q^2)_{ij} = \mathcal{O}(p^6), \quad (3.21)$$

$$\Pi_P^M(Q^2)_{ij} = \frac{2B_0 f_{ij}^2}{m_{ij}^2 + Q^2} + \mathcal{O}(p^6), \quad (3.22)$$

$$\Pi_S(Q^2)_{ij} = 8B_0^2(2L_8 + H_2) + \mathcal{O}(p^6), \quad (3.23)$$

$$\Pi_P(Q^2)_{ij} = \frac{2B_0^2 f_{ij}^2}{m_{ij}^2 + Q^2} + 8B_0^2(-2L_8 + H_2) + \mathcal{O}(p^6). \quad (3.24)$$

With m_{ij} the mass of the lightest pseudoscalar meson with flavour structure ij . These are obtained in the leading $1/N_c$ approximation so loop-effects are not needed. Notice that these expressions are valid to chiral order p^4 . From a term of the form $\text{tr}\{D_\mu \chi D^\mu \chi^\dagger\}$ there are contributions of order $(m_i - m_j)^2/Q^2$ to the vector two-point function $\Pi_V^{(0)}(Q^2)_{ij}$ and of order $(m_i - m_j)$ to the mixed scalar vector function $\Pi_S^M(Q^2)_{ij}$.

The functions $\Pi_A^{(0)}$, Π_P^M and Π_P get their leading behaviour from the pseudoscalar Goldstone pole. In addition $\Pi_A^{(1)}$ and $\Pi_A^{(0)}$ contain a kinematical pole at $Q^2 = 0$. The residue of the physical pole is proportional to the decay constant f_{ij} for the relevant meson, (for the $\bar{u}d$ ones, $f_{ud} \simeq f_\pi \simeq 92.5$ MeV). In χ PT, the constant B_0 is related to the vacuum expectation value in the chiral limit. In the large N_c limit and away from the chiral limit there are corrections due to the terms proportional to combination of $\mathcal{O}(p^4)$ couplings $2L_8 + H_2$ [16].

$$\langle 0 | : \bar{\Psi} \Psi : | 0 \rangle_{|\Psi=u,d,s} \equiv -f_0^2 B_0 (1 + \mathcal{O}(p^4)) . \quad (3.25)$$

The vacuum expectation value here, $\langle 0 | : \bar{\Psi} \Psi : | 0 \rangle$, is the one used in χ PT in the chiral limit and f_0 is the pseudoscalar meson decay constant in the chiral limit. The constants L_8 , L_{10} , H_1 and H_2 are coupling constants of the $\mathcal{O}(p^4)$ effective chiral Lagrangian in the notation of Gasser and Leutwyler [16]. The constants L_8 and L_{10} are known from the comparison between χ PT and low energy hadron phenomenology. At the scale of the ρ meson mass they are $L_8 = (0.9 \pm 0.3) \times 10^{-3}$ and $L_{10} = (-5.5 \pm 0.7) \times 10^{-3}$. The high energy constants H_1 and H_2 correspond to couplings which involve external source fields only and therefore can only be extracted from experiment given a prescription.

3.3 The method and Ward identities

The method used here is identical to the one used in [5]. The full two-point functions are the sum of diagrams like those in figure 2a. The one-loop two-point

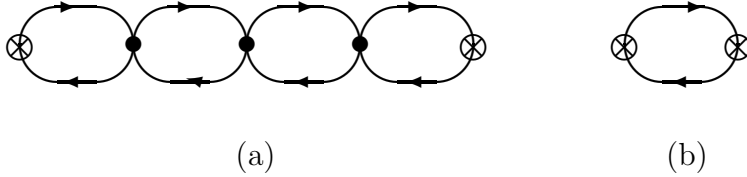


Figure 2: The graphs contributing to the two point-functions in the large N_c limit. a) The class of all strings of constituent quark loops. The four-fermion vertices are either $\mathcal{L}_{\text{NJL}}^{\text{S,P}}$ or $\mathcal{L}_{\text{NJL}}^{\text{V,A}}$ in eq. (2.2). The crosses at both ends are the insertion of the external sources. b) The one-loop case.

functions are those obtained by the graph in figure 2b. Using a recursion formula that relates the n -loop graph to a product of the one-loop and the $(n-1)$ -loop graph and the relevant combination of kinematic factors and G_V and G_S the whole class of graphs can be easily summed. Some care must be taken in the case where different two-point functions can mix so a matrix inversion is necessary (see ref. [5]).

The two-point functions defined above satisfy the following Ward identities. (We suppress the argument Q^2 for brevity.)

$$-Q^2 \Pi_V^{(0)}{}_{ij} = (m_i - m_j) \Pi_S^M{}_{ij}, \quad (3.26)$$

$$-Q^2 \Pi_S^M{}_{ij} = (m_i - m_j) \Pi_{Sij} + \langle \bar{q}_i q_i \rangle - \langle \bar{q}_j q_j \rangle, \quad (3.27)$$

$$-Q^2 \Pi_A^{(0)}{}_{ij} = (m_i + m_j) \Pi_P^M{}_{ij}, \quad (3.28)$$

$$-Q^2 \Pi_P^M{}_{ij} = (m_i + m_j) \Pi_{Pij} + \langle \bar{q}_i q_i \rangle + \langle \bar{q}_j q_j \rangle. \quad (3.29)$$

These are derived in the appendix B. From these the flavour symmetry of the mixed two-point functions can be derived from the vector ones.

The one-loop expressions, which we shall denote by $\bar{\Pi}$ and use further the same conventions as given for the full ones above are given in appendix C. They satisfy the same identities but with the current quark masses m_i replaced by the constituent ones, M_i . In addition to these, there are two more relations that follow in general if the one-loop part can be described by a heat-kernel expansion in terms of the quantities E and $R_{\mu\nu}$ of appendix B. These identities are (with the flavour subscript ij and argument suppressed)

$$\bar{\Pi}_V^{(1)} + \bar{\Pi}_V^{(0)} = \bar{\Pi}_A^{(1)} + \bar{\Pi}_A^{(0)}, \quad (3.30)$$

$$\bar{\Pi}_S + Q^2 \bar{\Pi}_V^{(0)} = \bar{\Pi}_P + Q^2 \bar{\Pi}_A^{(0)}. \quad (3.31)$$

3.4 The transverse vector sector

We introduce here for convenience an extra symbol g_V

$$g_V \equiv \frac{8\pi^2 G_V}{N_c \Lambda_\chi^2} Q^2. \quad (3.32)$$

The full resummed transverse vector two-point function is then

$$\Pi_V^{(1)}{}_{ij} = \frac{\bar{\Pi}_{Vij}^{(1)}}{1 + g_V \bar{\Pi}_{Vij}^{(1)}}. \quad (3.33)$$

This can be simply written in a form resembling the one in the complete VMD limit with couplings f_S , f_V and M_V depending on Q^2 and flavour and defined by

$$\Pi_V^{(1)}(Q^2)_{ij} = \frac{2f_S^2(Q^2)_{ij}}{Q^2} + \frac{2f_V^2(Q^2)_{ij} M_V^2(Q^2)_{ij}}{M_V^2(Q^2)_{ij} + Q^2}, \quad (3.34)$$

$$2f_S^2(Q^2)_{ij} = \frac{-Q^2 \bar{\Pi}_V^{(0)}(Q^2)_{ij}}{1 - g_V \bar{\Pi}_V^{(0)}(Q^2)_{ij}}, \quad (3.35)$$

$$2f_V^2(Q^2)_{ij} M_V^2(Q^2)_{ij} = \frac{N_c \Lambda_\chi^2}{8\pi^2 G_V} \frac{1}{1 - g_V \bar{\Pi}_V^{(0)}(Q^2)_{ij}}, \quad (3.36)$$

$$2f_V^2(Q^2)_{ij} = \bar{\Pi}_V^{(0+1)}(Q^2)_{ij}. \quad (3.37)$$

Where we have used the fact that (see appendices B and C) $\bar{\Pi}_V^{(0+1)} \equiv \bar{\Pi}_V^{(0)} + \bar{\Pi}_V^{(1)}$ has no pole at $Q^2 = 0$. There is a correction here (in $\bar{\Pi}_V^{(0)}$) due to the mixing with the scalar sector, which is allowed by the presence of explicit breaking of the vector symmetry (see the scalar mixed sector subsection 3.7). For the diagonal case, this is defined as $m_i = m_j$ or $M_i = M_j$, $\bar{\Pi}_V^{(0)}$ vanishes and the formulas above simplify very much.

The pole mass of the vector corresponds to the pole in this two point function or to the solution of $\text{Re}(Q^2 + M_V^2(Q^2)_{ij}) = 0$. Alternatively, one can define the VMD values for the vector parameters (f_V and M_V) as the best parameters of a linear fit of the inverse of $\Pi_V^{(1)}(Q^2)_{ij} - 2f_S^2(Q^2)_{ij}/Q^2$. These definitions have the advantage that they are also valid for the Euclidean region ($Q^2 > 0$) where the vector cannot decay into two constituent quarks. See sections on numerical applications 3.9 and Vector-Meson-Dominance 5 for further comments.

3.5 The transverse axial-vector sector

The transverse axial-vector two-point function derivation is also identical to the one in ref. [5].

$$\Pi_A^{(1)}{}_{ij} = \frac{\bar{\Pi}_{Aij}^{(1)}}{1 + g_V \bar{\Pi}_{Aij}^{(1)}}. \quad (3.38)$$

Using the identity (3.30) it can be seen that this has a pole at $Q^2=0$ because $\bar{\Pi}_A^{(0)}$ has it. As can be seen from the explicit expression and is proved in general in appendix B, the combination $\bar{\Pi}_V^{(0)} + \bar{\Pi}_V^{(1)}$ is regular at Q^2 going to zero. This again allows us to separate the pole at $Q^2 = 0$ in a simple fashion.

$$\Pi_A^{(1)}(Q^2)_{ij} = \frac{2f_{ij}^2(Q^2)}{Q^2} + \frac{2f_A^2(Q^2)_{ij}M_A^2(Q^2)_{ij}}{M_A^2(Q^2)_{ij} + Q^2}, \quad (3.39)$$

$$f_{ij}^2(Q^2) = g_A(Q^2)_{ij}\bar{f}_{ij}^2(Q^2), \quad (3.40)$$

$$2\bar{f}_{ij}^2(Q^2) = -Q^2\bar{\Pi}_A^{(0)}(Q^2)_{ij}, \quad (3.41)$$

$$\left(g_A(Q^2)_{ij}\right)^{-1} = 1 - g_V\bar{\Pi}_A^{(0)}(Q^2)_{ij}, \quad (3.42)$$

$$2f_A^2(Q^2)_{ij}M_A^2(Q^2)_{ij} = \frac{N_c\Lambda_\chi^2}{8\pi^2G_V}g_A(Q^2)_{ij}, \quad (3.43)$$

$$2f_A^2(Q^2)_{ij} = g_A^2(Q^2)_{ij}\bar{\Pi}_V^{(0+1)}(Q^2)_{ij}. \quad (3.44)$$

There is a correction here (in $\bar{\Pi}_A^{(0)}$) due to the mixing with the pseudo-scalar sector due to the presence of both spontaneous and explicit breaking of the axial-vector symmetry (see the pseudo-scalar mixed sector subsection). For further discussion of these expressions and the ones in the previous section we refer to the subsection 3.8 on Weinberg Sum Rules.

3.6 The pseudo-scalar mixed sector

The same method as used in [5] still applies with the results for the summed functions given in terms of the function $\Delta_P(Q^2)$ and the one loop two-point functions (with flavour subscripts ij suppressed),

$$\Pi_A^{(0)}(Q^2) = \frac{1}{\Delta_P(Q^2)} \left[(1 - g_S\bar{\Pi}_P(Q^2))\bar{\Pi}_A^{(0)}(Q^2) + g_S(\bar{\Pi}_P^M(Q^2))^2 \right], \quad (3.45)$$

$$\Pi_P^M(Q^2) = \frac{1}{\Delta_P(Q^2)}\bar{\Pi}_P^M(Q^2), \quad (3.46)$$

$$\Pi_P(Q^2) = \frac{1}{\Delta_P(Q^2)} \left[(1 - g_V\bar{\Pi}_A^{(0)}(Q^2))\bar{\Pi}_P(Q^2) + g_V(\bar{\Pi}_P^M(Q^2))^2 \right], \quad (3.47)$$

$$\Delta_P(Q^2) = \left(1 - g_V\bar{\Pi}_A^{(0)}(Q^2)\right) \left(1 - g_S\bar{\Pi}_P(Q^2)\right) - g_Sg_V(\bar{\Pi}_P^M(Q^2))^2. \quad (3.48)$$

Using the identities for the one-loop case it can be shown that the resummed ones satisfy the Ward identities of appendix B with the current quark masses. To show this it is also necessary to use the Schwinger-Dyson equation for the constituent quark masses in eq.(2.3).

In order to rewrite this in terms of a nicer notation we first express $\Delta_P(Q^2)_{ij}$ in a different form using the identities for the one-loop two-point functions.

$$\Delta_P(Q^2)_{ij} = \frac{g_S \bar{\Pi}_P^M(Q^2)_{ij}}{M_i + M_j} (m_{ij}^2(Q^2) + Q^2) \quad (3.49)$$

$$\text{with } m_{ij}^2(Q^2) \equiv \frac{(m_i + m_j)}{g_S g_A(Q^2) \bar{\Pi}_P^M(Q^2)_{ij}}. \quad (3.50)$$

Inserting the definition of $f_{ij}^2(Q^2)$ and $1/g_S = -\langle \bar{q}_i q_i \rangle / (M_i - m_i)$ we recover the Gell-Mann–Oakes–Renner (GMOR) relation for the pion mass [17] when eq. (3.50) is expanded in powers of m_i . For further discussion on corrections to the GMOR relation in this model we refer to the section on numerical applications 3.9. Formula (3.50) gives the expression for the pole due to the lightest pseudoscalar mesons in the presence of explicit chiral symmetry breaking.

This then allows us to rewrite the full two-point functions in a very simple fashion:

$$\Pi_A^{(0)}(Q^2)_{ij} = 2f_{ij}^2(Q^2) \left(\frac{1}{m_{ij}^2(Q^2) + Q^2} - \frac{1}{Q^2} \right), \quad (3.51)$$

$$\Pi_P^M(Q^2)_{ij} = \frac{M_i + M_j}{g_S} \frac{1}{m_{ij}^2(Q^2) + Q^2}, \quad (3.52)$$

$$\Pi_P(Q^2)_{ij} = -\frac{1}{g_S} + \frac{(M_i + M_j)^2}{2f_{ij}^2(Q^2)} \frac{1}{g_S^2} \frac{1}{m_{ij}^2(Q^2) + Q^2}. \quad (3.53)$$

Here we want to point out that the two-point functions Π_P^M and Π_P suffer from the same ambiguity (via its dependence on g_S) as the quark-antiquark one point-function (see discussion at the end of section 2) when compared with the χ PT results.

3.7 The scalar mixed sector

Here we have to extend the analysis of [5] to include possible mixing effects. This can be done in the same way as in the previous subsection with the result (with flavour subscripts ij suppressed),

$$\Pi_V^{(0)}(Q^2) = \frac{1}{\Delta_S(Q^2)} \left[(1 - g_S \bar{\Pi}_S(Q^2)) \bar{\Pi}_V^{(0)}(Q^2) + g_S (\bar{\Pi}_S^M(Q^2))^2 \right], \quad (3.54)$$

$$\Pi_S^M(Q^2) = \frac{1}{\Delta_S(Q^2)} \bar{\Pi}_S^M(Q^2), \quad (3.55)$$

$$\Pi_S(Q^2) = \frac{1}{\Delta_S(Q^2)} \left[(1 - g_V \bar{\Pi}_V^{(0)}(Q^2)) \bar{\Pi}_S(Q^2) + g_V (\bar{\Pi}_S^M(Q^2))^2 \right], \quad (3.56)$$

$$\Delta_S(Q^2) = \left(1 - g_V \bar{\Pi}_V^{(0)}(Q^2) \right) \left(1 - g_S \bar{\Pi}_S(Q^2) \right) - g_S g_V (\bar{\Pi}_S^M(Q^2))^2. \quad (3.57)$$

To rewrite this in a simple fashion we would again like to expand Δ_S in a simple pole like fashion. Using the identities for the one-loop two-point functions this can almost be done, we obtain

$$\begin{aligned} \Delta_S(Q^2)_{ij} &= \frac{g_S \bar{\Pi}_P^M(Q^2)_{ij}}{M_i + M_j} \left((M_i + M_j)^2 + g_A(Q^2)_{ij} m_{ij}^2(Q^2) + Q^2 \right) \\ &+ \bar{\Pi}_V^{(0)}(Q^2)_{ij} \left(Q^2 g_S - g_V \frac{m_i - m_j}{M_i - M_j} \right). \end{aligned} \quad (3.58)$$

It can be seen that in the diagonal case a simple expression for the scalar meson pole can be found,

$$M_S^2(-M_S^2) \Big|_{m_i=m_j} = (M_i + M_j)^2 + g_A(-M_S^2)_{ii} m_{ii}^2(-M_S^2). \quad (3.59)$$

The expression for the scalar two-point function $\Pi_S(Q^2)$ is in this case

$$\Pi_S(Q^2) \Big|_{m_i=m_j} = \left\{ -\frac{1}{g_S} + \frac{g_A(Q^2)_{ij} (M_i + M_j)^2}{2f_{ij}^2(Q^2)} \frac{1}{g_S^2} \frac{1}{M_S^2(Q^2) + Q^2} \right\}_{m_i=m_j} \quad (3.60)$$

So in the diagonal case a simple relation between the scalar mass, the constituent masses and the pseudoscalar mass remains valid to all orders in the masses. In this case $\Pi_V^{(0)} = \Pi_S^M = 0$.

For the off-diagonal case, i.e. $m_i \neq m_j$, the corresponding expressions for $\Pi_V^{(0)}$, Π_S^M and Π_S can be obtained from eqs. (3.54)-(3.57) and the explicit $\bar{\Pi}$ functions in appendix C. There is a small shift in the pole compared to eq. (3.59) for the case $m_i \neq m_j$. From appendix C, in eq. (C.4), it can be seen that $\bar{\Pi}_V^{(0)}$ itself has a zero close to a value of $Q^2 = M_S^2$ of eq. (3.59). In addition $\bar{\Pi}_V^{(0)}$ is suppressed by $(M_i - M_j)^2 / Q^2$. Therefore the value of the pole in the off-diagonal case is not too far from that in eq. (3.59).

Here we want to point out that (as in the mixed pseudoscalar sector) the two-point functions $\Pi_V^{(0)}$, Π_S^M and Π_S suffer from the same ambiguity (via its dependence on g_S) as the quark-antiquark one point-function (see discussion at the end of section 2) when compared with the χ PT results.

3.8 Weinberg Sum Rules

The Weinberg Sum Rules are general restrictions on the short-distance behaviour of various two-point functions [18]. They were first discussed within QCD in

ref. [19]. A low-energy model of QCD should have a behaviour at intermediate energies that matches on reasonably well with the QCD behaviour. The general behaviour should be ($\Pi_{LR} \equiv \Pi_V - \Pi_A$)

$$\lim_{Q^2 \rightarrow \infty} \left(Q^2 \Pi_{LR}^{(0+1)}(Q^2) \right) = 0 \quad \text{First WSR} , \quad (3.61)$$

$$\lim_{Q^2 \rightarrow \infty} \left(Q^4 \Pi_{LR}^{(1)}(Q^2) \right) = 0 \quad \text{Second WSR} , \quad (3.62)$$

$$\lim_{Q^2 \rightarrow \infty} \left(Q^4 \Pi_{LR}^{(0)}(Q^2) \right) = 0 \quad \text{Third WSR} . \quad (3.63)$$

Let us review first the QCD behaviour of these Sum Rules. In the large N_c limit the three WSRs are theorems of QCD in the chiral limit (i.e., $\mathcal{M} \rightarrow 0$). The first WSR is still fulfilled in the large N_c limit with non-vanishing current quark masses. However the second and the third ones are violated as follows [20],

$$\begin{aligned} \lim_{Q^2 \rightarrow \infty} \left(Q^4 \Pi_{LR}^{(1)}(Q^2) \right) &= - \lim_{Q^2 \rightarrow \infty} \left(Q^4 \Pi_{LR}^{(0)}(Q^2) \right) \\ &= 2 (m_i \langle \bar{q}_j q_j \rangle + m_j \langle \bar{q}_i q_i \rangle) . \end{aligned} \quad (3.64)$$

As shown in [5] the class of ENJL-like models does satisfy the three WSRs in the chiral limit. We shall now check how well this does in the case of explicit breaking of chiral symmetry.

The high-energy behaviour of the two-point functions $\Pi_{V,A}^{(0,1)}$ needed for the three WSRs can be easily obtained from the expressions in sections 3.4, 3.5, 3.6 and 3.7. The first and second WSRs are satisfied in these ENJL-like models even with non-vanishing and all different current quark-masses. The high energy behaviour (Q^4) of these models is thus too strongly suppressed for $\Pi_{LR}^{(1)}(Q^2)$ to reproduce the QCD behaviour in the second WSR. The third one is violated as in QCD and one has

$$\lim_{Q^2 \rightarrow \infty} \left(Q^4 \Pi_{LR}^{(0)}(Q^2) \right) = \frac{2}{g_S} (m_i M_j + m_j M_i) . \quad (3.65)$$

Let us now see what relations between low-energy hadronic couplings do these Sum Rules imply for this ENJL cut-off model. In the equal mass sector, $m_i = m_j \neq 0$, one has

$$f_V^2 M_V^2 = f_A^2 M_A^2 + f_\pi^2 , \quad (3.66)$$

$$f_V^2 M_V^4 = f_A^2 M_A^4 . \quad (3.67)$$

Remember that in QCD one has in this case

$$f_V^2 M_V^2 = f_A^2 M_A^2 + f_\pi^2 , \quad (3.68)$$

$$f_V^2 M_V^4 = f_A^2 M_A^4 + m_\pi^2 f_\pi^2 . \quad (3.69)$$

In the off-diagonal case, $m_i \neq m_j$, the situation becomes a lot more complicated. However, since the off-diagonal part is suppressed by $(M_i - M_j)^2/Q^2$ one does not expect qualitatively different results.

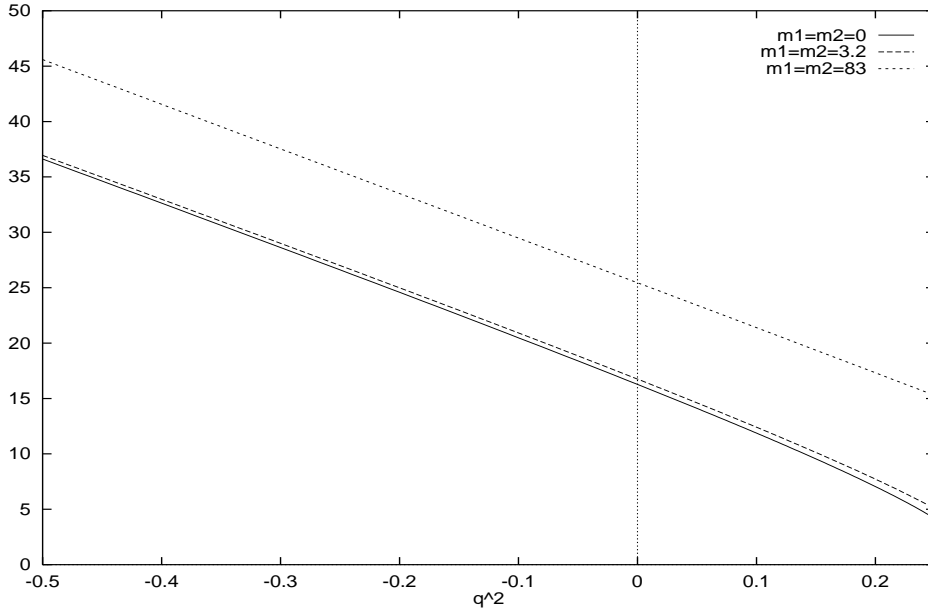


Figure 3: The inverse of the transverse vector two-point function for equal quark masses in the chiral limit, i.e. $\mathcal{M} \rightarrow 0$; for the ρ meson, i.e. $m_1 = m_2 = 3.2$ MeV and for the ϕ meson, i.e. $m_1 = m_2 = 83$ MeV. The units of q^2 are GeV^2

3.9 Some numerical results

As can be seen from the explicit formulas the change with respect to ref. [5] is in most cases a (small) shift in the two-point function mass pole positions. Therefore we do not plot too many of the two-point functions. As numerical input we use for G_S , G_V and Λ_χ the values from fit 1 in ref. [4]. These are $\Lambda_\chi = 1.160$ GeV and $G_S = 1.216$. The value of $g_A(Q^2 = 0)$ there was 0.61. This is $G_V = 1.263$. For the current quark masses we use the value of the quark mass for $\bar{m} \equiv m_u = m_d$ that reproduces the physical neutral pion and kaon masses. With the other parameters as fixed above this is $\bar{m} = 3.2$ MeV and $m_s/\bar{m} = 26$.

As an example we have plotted the inverse of the transverse vector two-point function in eq. (3.34) in figure 3 for the values of G_S and Λ_χ corresponding above mentioned. The full curve is the result in the chiral limit ($\mathcal{M} \rightarrow 0$) and the dashed is the result with $m_i = m_j = \bar{m}$ the value above. The reason we have plotted the inverse will become clear in section 5. We also show the inverse for $m_i = m_j = m_s$ the value above in the short-dashed curve. To show the result for unequal quark masses we have plotted in figure 4 the transverse vector two-point function itself for the chiral limit case and for the $\bar{u}s$ case with m_s and \bar{m} above. Notice that the two-point function now has a kinematical pole at $q^2 = 0$.

We have also plotted in figure 5 for the parameters quoted above the dependence of the pion mass on Q^2 . Since $f_{ij}^2 m_{ij}^2$ is a constant, see eq. (3.50) this is also the Q^2 dependence of the inverse of the f_{ij} decay constant squared.

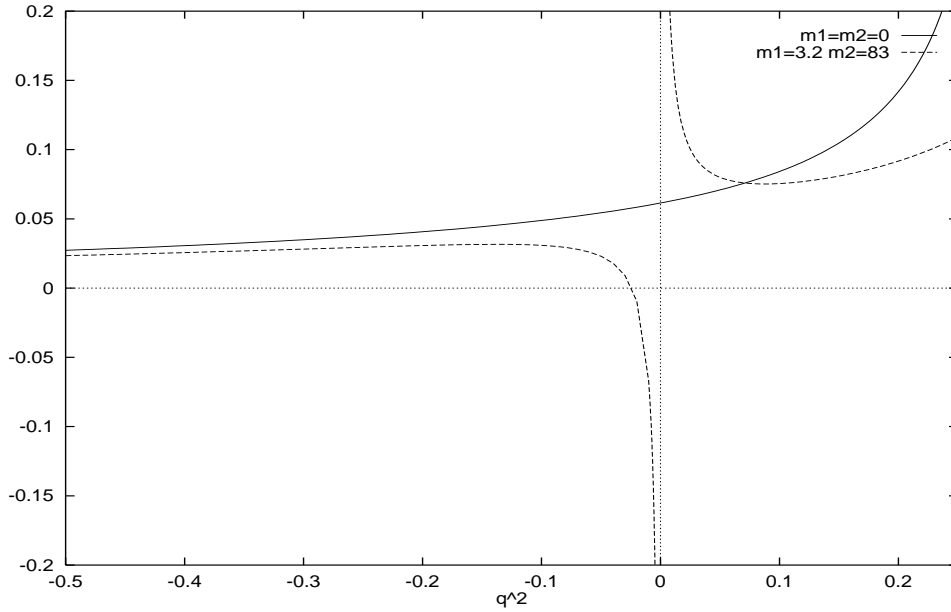


Figure 4: The transverse vector-two-point function for the chiral limit and for unequal quark masses, $m_1 = \bar{m}$ and $m_2 = m_s$. Note the kinematical pole at $q^2 = 0$. The units of q^2 are GeV^2 .

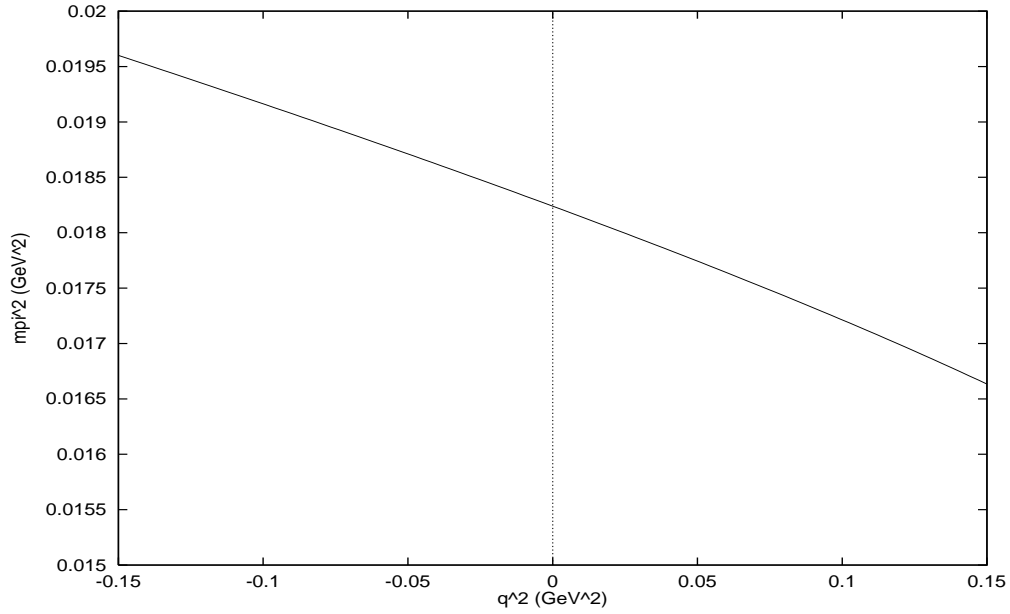


Figure 5: The running pseudoscalar mass squared, $m_{ij}^2(-q^2)$, as a function of q^2 for $m_i = m_j = 3.2 \text{ MeV}$.

Let us make some comments on the corrections we find to the GMOR relation (3.50) in this model. The corrections to the GMOR relation [17] can be calculated here in an analogous expansion to the one in χ PT. Then the GMOR relation can be written as follows [16] (for the diagonal flavour case, i.e. $i = j$)

$$2m_i \langle \bar{q}_i q_i \rangle = -m_{ii}^2(-q^2) f_{ii}^2(-q^2) \left(1 - 4 \frac{m_{ii}^2(0)}{f_{ii}^2(0)} (2L_8 - H_2) + \mathcal{O}(p^6) \right). \quad (3.70)$$

Here we have included all the chiral corrections to the quark condensate, to the pion mass and to the pion decay constant in their respective values. Then the remaining is a correction to the GMOR relation. We have also calculated this correction in this model and it turns out to be

$$4 \frac{m_{ii}^2(0)}{f_{ii}^2(0)} (2L_8 - H_2) + \mathcal{O}(p^6) = \frac{m_i}{M_i}. \quad (3.71)$$

Notice that the r.h.s. contains all the orders in the χ PT expansion in the large N_c limit. Numerically, this correction is around 1 % for pions and 20 % for kaons and approximately agrees with the one found in QCD Sum Rules [21]. For the combination of $\mathcal{O}(p^4)$ couplings $2L_8 - H_2$ in this model we get

$$2L_8 - H_2 = \frac{N_c}{16\pi^2} \frac{g_A^2(0)}{2} \frac{\Gamma^2(0, \epsilon)}{\Gamma(-1, \epsilon)}, \quad (3.72)$$

with $\epsilon = M^2/\Lambda_\chi^2$ and M the constituent quark mass in the chiral limit. (For definitions of the incomplete Gamma functions $\Gamma(n, \epsilon)$ see appendix A.) The expression in (3.72) is the one consistent with the use of Ward identities to sum the infinite string of constituent quark bubbles. Numerically we get $2L_8 - H_2 \simeq 1.3 \cdot 10^{-3}$ for the input parameters above. This differs from the one found at the one-loop level, in this same model in ref. [4] (see footnote ¹), numerically they find $2L_8 - H_2 = 0.2 \cdot 10^{-3}$.

4 Some three-point functions

4.1 VPP with the use of the Ward identities

In this subsection we calculate the Vector Pseudoscalar Pseudoscalar (VPP) three-point function to all orders in χ PT using the same type of methods as those used for the two-point functions. The three-point function we calculate is the following

$$\Pi_\mu^{VPP}(p_1, p_2) \equiv i^2 \int d^4x \int d^4y e^{i(p_1 \cdot x + p_2 \cdot y)} \langle 0 | T \left(V_\mu^{ij}(0) P^{kl}(x) P^{mn}(y) \right) | 0 \rangle. \quad (4.1)$$

Where i, j, k, l, m and n are flavour indices. In the limit of large N_c the flavour structure is limited because of Zweig's rule (this flavour structure is general for any three-point function of three quark currents),

$$\Pi_\mu^{VPP}(p_1, p_2) \equiv \Pi_\mu^+(p_1, p_2)_{ikm} \delta_{il} \delta_{kn} \delta_{mj} + \Pi_\mu^-(p_1, p_2)_{ikm} \delta_{in} \delta_{kj} \delta_{ml} . \quad (4.2)$$

Bose symmetry requires that

$$\Pi_\mu^+(p_1, p_2)_{ikm} = \Pi_\mu^-(p_2, p_1)_{imk} . \quad (4.3)$$

The three-point function $\Pi_\mu^{VPP}(p_1, p_2)$ can then be simply calculated by only taking one particular flavour combination. Finally we can use Lorentz-invariance to rewrite

$$\Pi_\mu^+(p_1, p_2)_{ikm} = p_{1\mu} \Pi_{ikm}^A(p_1^2, p_2^2, q^2) + p_{2\mu} \Pi_{ikm}^B(p_1^2, p_2^2, q^2) , \quad (4.4)$$

where we have defined $q \equiv p_1 + p_2$.

We shall limit ourselves to the vector diagonal case, i.e. $m_i = m_j$. In the vector off-diagonal case there will also be non-trivial mixings with the scalar-pseudoscalar-pseudoscalar three-point function. Here a relatively simple Ward identity for this three-point function can be derived from $\partial^\mu V_\mu^{ij} = 0$ and the equal-time commutation relations. It is

$$q^\mu \Pi_\mu^+(p_1, p_2)_{ikm} = -\Pi_P(-p_1^2)_{ki} + \Pi_P(-p_2^2)_{mk} . \quad (4.5)$$

So the Ward identity relates the three-point function to a combination of two-point functions. This determines one of the two functions Π^A, Π^B in terms of the other. The Ward identity gives, for instance, the following constraint (for $p_1^2 = p_2^2$ and $i = m$)

$$\Pi_{iki}^B(p^2, p^2, q^2) = -\Pi_{iki}^A(p^2, p^2, q^2) . \quad (4.6)$$

The type of graphs that need to be summed are depicted in figure 6. Each of the three tails here is the diagram in figure 2a with the same explanation as there. We have there depicted one particular flavour combination. This is the one that corresponds to the function Π_μ^+ given above. The i, k, m written above the lines are the flavours of each line.

All graphs are formed by having the tails summed over $0, 1, 2, \dots, \infty$ loops connected by four-fermion couplings. These then couple to the one-loop three-point function (or vertex) $\bar{\Pi}_\mu^+$, with various possibilities for the insertion in the three-point vertex. These possibilities for the γ -matrices are written in figure 6 inside the main loop.

In this figure the left-hand side depicts the insertion of the current $V_\mu^{ij}(0)$ and Tail I is the connection to this current. On the end connecting to the one-loop three-point function it is only nonzero for another vector insertion since in the

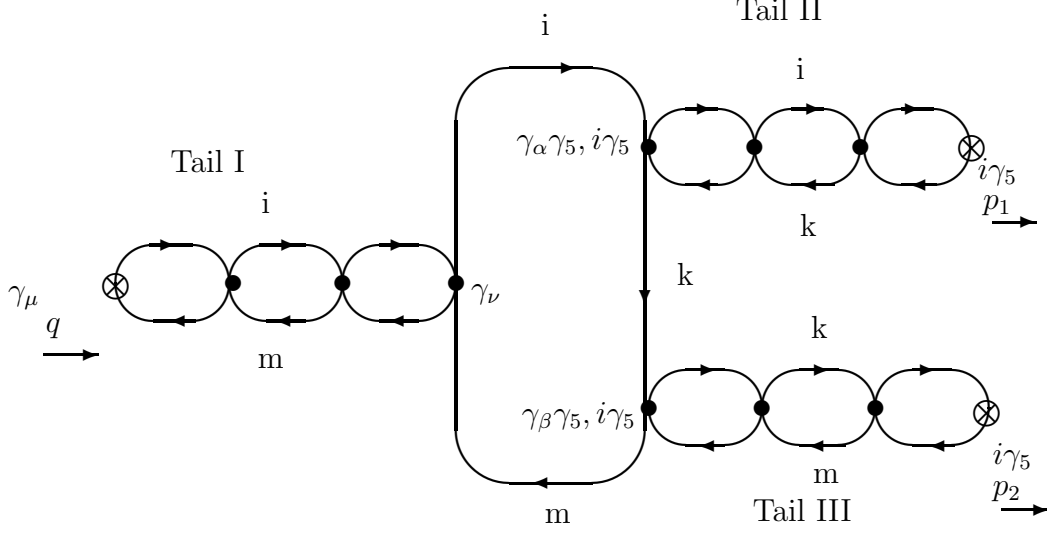


Figure 6: The graphs that need to be summed in the large N_c limit for the Vector-Pseudoscalar-Pseudoscalar three-point function. See text for explanation.

diagonal case we consider, the mixed vector–scalar two-point function vanishes. Its expression is given by

$$g_{\mu\nu} + \frac{-8\pi^2 G_V}{N_c \Lambda_\chi^2} \Pi_{\mu\nu}^V(-q^2)_{mi} . \quad (4.7)$$

Here the first term comes from where the external current directly connects to the one-loop three-point function and the second term is with the two-point function in between. The sum of both is

$$\frac{g_{\mu\nu} M_V^2(-q^2)_{mi} - q_\mu q_\nu}{M_V^2(-q^2)_{mi} - q^2} . \quad (4.8)$$

A similar discussion can be done for Tail II and Tail III. First we have the insertion of the current $P^{kl}(x)$ at the external end. On the end connecting to the one-loop three-point function we can have $i\gamma_5$ or an axial-vector insertion since the mixed axial-vector–pseudoscalar two-point function is nonzero. The $i\gamma_5$ insertion tail is :

$$\begin{aligned} & 1 + \frac{4\pi^2 G_S}{N_c \Lambda_\chi^2} \Pi_P(-p_1^2)_{ki} \\ &= \frac{(M_k + M_i)^2}{2g_S f_{ki}^2(-p_1^2)(m_{ki}^2(-p_1^2) - p_1^2)} . \end{aligned} \quad (4.9)$$

For the connection with the axial-vector insertion it is instead

$$\begin{aligned} & \frac{8\pi^2 G_V}{N_c \Lambda_\chi^2} i p_1^\alpha \Pi_P^M(-p_1^2)_{ki} \\ &= \frac{i p_1^\alpha}{2 f_V^2 M_V^2} \frac{(M_k + M_i)}{g_S (m_{ki}^2(-p_1^2) - p_1^2)}. \end{aligned} \quad (4.10)$$

The combination $f_V^2 M_V^2$ is here flavour and p_1^2 independent, it is the combination in eq. (3.36) with $\bar{\Pi}_V^{(0)}(Q^2)_{ij} = 0$ since we are in the diagonal flavour case. The way both these types of insertions can appear due to the tail are how within this formulation the mixing of pseudoscalar and axial-vector degrees comes about. These will be described by factors of g_A^2 (see below). Tail III is identical to Tail II with the substitutions $p_1 \rightarrow p_2$ and $i, k \rightarrow k, m$.

The full expression for Π_μ^+ is

$$\begin{aligned} \Pi^{+\mu}(p_1, p_2) = & \left\{ g^{\mu\nu} + \frac{-8\pi^2 G_V}{N_c \Lambda_\chi^2} \Pi^{V\mu\nu}(-q^2)_{mi} \right\} \\ & \times \left\{ \bar{\Pi}_\nu^+(p_1, p_2) \left(1 + \frac{4\pi^2 G_S}{N_c \Lambda_\chi^2} \Pi_P(-p_1^2)_{ki} \right) \left(1 + \frac{4\pi^2 G_S}{N_c \Lambda_\chi^2} \Pi_P(-p_2^2)_{mk} \right) \right. \\ & + \bar{\Pi}_{\nu\beta}^{VPA}(p_1, p_2) \left(1 + \frac{4\pi^2 G_S}{N_c \Lambda_\chi^2} \Pi_P(-p_1^2)_{ki} \right) \left(\frac{8\pi^2 G_V}{N_c \Lambda_\chi^2} i p_2^\beta \Pi_P^M(-p_2^2)_{mk} \right) \\ & + \bar{\Pi}_{\nu\alpha}^{VAP}(p_1, p_2) \left(\frac{8\pi^2 G_V}{N_c \Lambda_\chi^2} i p_1^\alpha \Pi_P^M(-p_1^2)_{ki} \right) \left(1 + \frac{4\pi^2 G_S}{N_c \Lambda_\chi^2} \Pi_P(-p_2^2)_{mk} \right) \\ & \left. + \bar{\Pi}_{\nu\alpha\beta}^{VAA}(p_1, p_2) \left(\frac{8\pi^2 G_V}{N_c \Lambda_\chi^2} i p_1^\alpha \Pi_P^M(-p_1^2)_{ki} \right) \left(\frac{8\pi^2 G_V}{N_c \Lambda_\chi^2} i p_2^\beta \Pi_P^M(-p_2^2)_{mk} \right) \right\}. \end{aligned} \quad (4.11)$$

Where the one-loop three-point functions $\bar{\Pi}_{\mu\nu}^{VPA}$, $\bar{\Pi}_{\mu\nu}^{VAP}$ and $\bar{\Pi}_{\mu\nu\alpha}^{VAA}$ are the one fermion-loop result for

$$\Pi_{\mu\nu}^{VPA}(p_1, p_2) \equiv i^2 \int d^4x \int d^4y e^{i(p_1 \cdot x + p_2 \cdot y)} \langle 0 | T \left(V_\mu^{im}(0) P^{ki}(x) A_\nu^{mk}(y) \right) | 0 \rangle, \quad (4.12)$$

$$\Pi_{\mu\nu}^{VAP}(p_1, p_2) \equiv i^2 \int d^4x \int d^4y e^{i(p_1 \cdot x + p_2 \cdot y)} \langle 0 | T \left(V_\mu^{im}(0) A_\nu^{ki}(x) P^{mk}(y) \right) | 0 \rangle, \quad (4.13)$$

$$\Pi_{\mu\nu\alpha}^{VAA}(p_1, p_2) \equiv i^2 \int d^4x \int d^4y e^{i(p_1 \cdot x + p_2 \cdot y)} \langle 0 | T \left(V_\mu^{im}(0) A_\nu^{ki}(x) A_\alpha^{mk}(y) \right) | 0 \rangle. \quad (4.14)$$

To obtain the full expression in eq. (4.11) it now remains to calculate these VPP, VAP, VPA and VAA one-loop three-point functions (or vertices). The axial-vector ones always come multiplied with the relevant momentum. So we always have the scalar products $p_1 \cdot A^{ki}(x)$ and $p_2 \cdot A^{mk}(y)$. That means that

using the Ward identities we can relate the VAA, VAP, VPA to the VPP one plus possibly two-point function terms resulting from equal time commutators.

These Ward identities are (remember we assume $M_i = M_j$ here).

$$\begin{aligned}
ip_1^\nu \bar{\Pi}_{\mu\nu\alpha}^{VAA}(p_1, p_2) &= -(M_k + M_i) \bar{\Pi}_{\mu\alpha}^{VPA}(p_1, p_2) \\
&\quad - \bar{\Pi}_{\mu\alpha}^V(-q)_{mi} + \bar{\Pi}_{\mu\alpha}^A(-p_2)_{mk} ; \tag{4.15}
\end{aligned}$$

$$\begin{aligned}
ip_1^\nu \bar{\Pi}_{\mu\nu}^{VAP}(p_1, p_2) &= -(M_k + M_i) \bar{\Pi}_\mu^+(p_1, p_2) \\
&\quad + i \bar{\Pi}_{P\mu}(-p_2)_{mk} . \tag{4.16}
\end{aligned}$$

The other needed ones can be derived from this using Bose-symmetry. Notice that there is no contribution here from the flavour chiral anomaly (see eq. (4.24)).

We can now use these identities to obtain the final result for the three-point function we want. The terms which after the use of the one-loop identities above are proportional to VPP can be combined into a simple form using $g_A(p^2)$. The result is (we have $M_i = M_j$ and $j = m$ in this flavour configuration).

$$\begin{aligned}
\Pi^{+\mu}(p_1, p_2) &= \\
&\quad \left(\frac{(M_i + M_k)^4}{4g_S^2 f_{ki}^2(-p_1^2) f_{mk}^2(-p_2^2)} \right) \left(\frac{g^{\mu\nu} M_V^2(-q^2)_{mi} - q^\mu q^\nu}{M_V^2(-q^2)_{mi} - q^2} \right) \\
&\quad \times \frac{1}{(m_{ki}^2(-p_1^2) - p_1^2)(m_{mk}^2(-p_2^2) - p_2^2)} \left\{ g_A(-p_1^2)_{ki} g_A(-p_2^2)_{mk} \bar{\Pi}_\nu^+(p_1, p_2) \right. \\
&\quad + \frac{(1 - g_A(-p_1^2)_{ki})(1 - g_A(-p_2^2)_{mk})}{(M_i + M_k)^2} \{ (p_2 \cdot q) p_{1\nu} - (p_1 \cdot q) p_{2\nu} \} \bar{\Pi}_V^{(1)}(-q^2)_{mi} \\
&\quad - \frac{g_A(-p_1^2)_{ki}(1 - g_A(-p_2^2)_{mk})}{M_i + M_k} p_{1\nu} \bar{\Pi}_P^M(-p_1^2)_{ki} \\
&\quad \left. + \frac{g_A(-p_2^2)_{mk}(1 - g_A(-p_1^2)_{ki})}{M_i + M_k} p_{2\nu} \bar{\Pi}_P^M(-p_2^2)_{mk} \right\} . \tag{4.17}
\end{aligned}$$

This result satisfies the Ward identity (4.5) if the one-loop function $\bar{\Pi}_\mu^+$ one satisfies the same one with the one-loop functions. This provides a rather non-trivial check on the result (4.17).

It now only remains to calculate the one-loop form factor $\bar{\Pi}_\mu^+(p_1, p_2)$. We give its expression in appendix D. At this point we can see in eq. (4.17) how far regularization ambiguities affect the result. We first have to define the two-point functions. Here all ambiguities are restricted to two bare functions (see section 3 for details). This three-point function adds one more in general, the three-propagator function $I_3(p_1^2, p_2^2, q^2)$ (see explicit expression in appendix D). Of course, this one-loop form factor $\bar{\Pi}_\mu^+(p_1, p_2)$, satisfies all the identities eqs. (4.1) to (4.6) as well. We refer to section 5.2 for the definition of the physical vector form factor after reducing this VPP three-point function. We shall also discuss there the VMD limit in this form factor and give some numerics.

The same three-point function can be calculated in Chiral Perturbation Theory. The result is

$$\Pi^{+\mu}(p_1, p_2) = \frac{2B_0^2 f_{mi}^2}{(m_{ki}^2 - p_1^2)(m_{mk}^2 - p_2^2)} (p_2 - p_1)^\mu \left(1 + \frac{2L_9}{f_{mi}^2} q^2 + \mathcal{O}(p^6) \right). \quad (4.18)$$

Pulling out the pion poles (see section 5.2 for technical details) and taking the low-energy limit and the value of L_9 in this class of models our full result in eq. (4.17) reduces to this, providing one more non-trivial check.

4.2 PVV with a discussion about its Ward identity

In this subsection we calculate the Pseudoscalar Vector Vector (PVV) three-point function to all orders in χ PT with the same method as the one used before.

$$\Pi_{\mu\nu}^{PVV}(p_1, p_2) \equiv i^2 \int d^4x \int d^4y e^{i(p_1 \cdot x + p_2 \cdot y)} \langle 0 | T \left(P^{ij}(0) V_\mu^{kl}(x) V_\nu^{mn}(y) \right) | 0 \rangle. \quad (4.19)$$

Where i, j, k, l, m and n are flavour indices. A similar discussion about the structure due to Zweig's rule can be given as was done before. We do the analogous decomposition into $\Pi_{\mu\nu}^+$ and $\Pi_{\mu\nu}^-$ functions as was done for the three-point function VPP (see previous section). We shall here restrict ourselves to the case where all current masses or constituent masses are equal. Our main aim in this subsection is to show how the flavour anomaly [22] affects the use of the one-loop identities.

The class of graphs needed here is shown in figure 7 for the Π^+ flavour combination. Each of the three tails here is the diagram in figure 2a with the same explanation as there. The vector-like tails, II and III, can be easily summed (see discussion for the summation of the vector tail in the previous section) to obtain the overall factors

$$g_{\mu\alpha} + \frac{-8\pi^2 G_V}{N_c \Lambda_\chi^2} \Pi_{\mu\alpha}^V(-p_1^2) \quad (4.20)$$

and

$$g_{\nu\beta} + \frac{-8\pi^2 G_V}{N_c \Lambda_\chi^2} \Pi_{\nu\beta}^V(-p_2^2). \quad (4.21)$$

Tail I can again couple at the one-loop end to both an axial-vector and pseudoscalar two-point function. These have the same form as equations (4.9) and (4.10) in the previous section with $p_1 \rightarrow q$. Summing up the three tails the total result is then

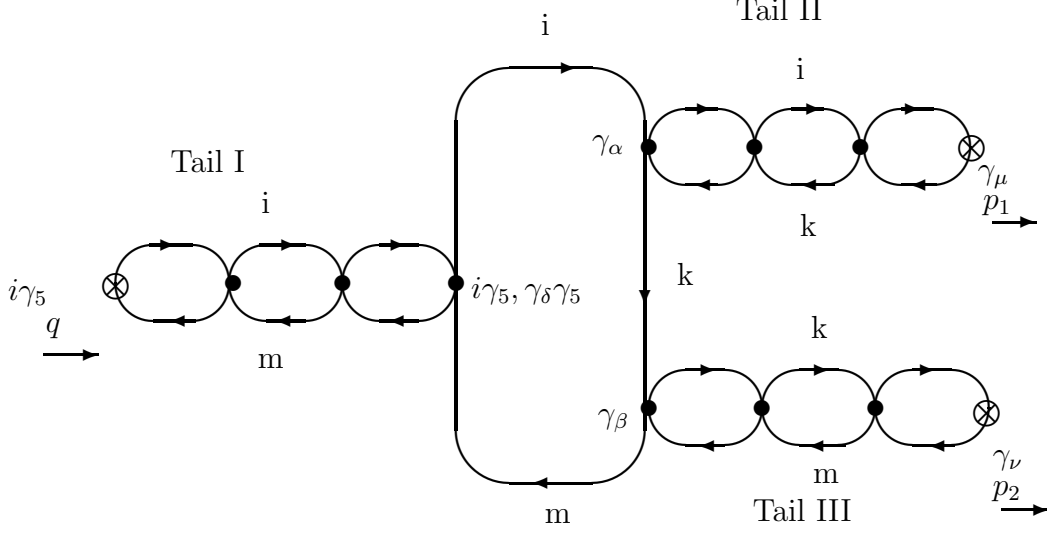


Figure 7: The graphs that need to be summed in the large N_c limit for the Pseudoscalar-Vector-Vector three-point function. See text for explanation.

$$\begin{aligned}
\Pi^{+\mu\nu}(p_1, p_2) = & \left(g^{\mu\alpha} + \frac{-8\pi^2 G_V}{N_c \Lambda_\chi^2} \Pi^{V\mu\alpha}(-p_1^2) \right) \left(g^{\nu\beta} + \frac{-8\pi^2 G_V}{N_c \Lambda_\chi^2} \Pi^{V\nu\beta}(-p_2^2) \right) \\
& \times \left[\bar{\Pi}_{\alpha\beta}^+(p_1, p_2) \left\{ 1 + \frac{4\pi^2 G_S}{N_c \Lambda_\chi^2} \Pi_P(-q) \right\} + \bar{\Pi}_{\rho\alpha\beta}^{AVV}(p_1, p_2) \left(\frac{8\pi^2 G_V}{N_c \Lambda_\chi^2} i q^\rho \Pi_P^M(-q) \right) \right]
\end{aligned} \tag{4.22}$$

with $\bar{\Pi}_{\alpha\mu\nu}^{AVV}$ the one-loop result for the following three-point function

$$\Pi_{\rho\mu\nu}^{AVV}(p_1, p_2) \equiv i^2 \int d^4x \int d^4y e^{i(p_1 \cdot x + p_2 \cdot y)} \langle 0 | T \left(A_\rho^{im}(0) V_\mu^{ki}(x) V_\nu^{mk}(y) \right) | 0 \rangle . \tag{4.23}$$

The main new part here is that at the one-loop level we now have to include the anomalous part of the Ward identities. There has been in fact quite some confusion whether this can be done consistently. We have shown how this subtraction needs to be done in the case of ENJL-like models in ref. [9]. The anomaly itself in this class of models is not well defined but a consistent subtraction procedure to obtain the QCD flavour anomaly can be easily formulated, see ref. [9]. We could in principle use the prescription of ref. [9] directly to obtain the

one-loop three-point function. Here we want to apply it to the PVV three-point function to all orders in external momenta and quark masses. The prescription is essentially to use the anomalous QCD Ward identities for the axial current consistently. We shall use the scheme where vector currents are conserved [23]. The subtractions these Ward identities impose in order to reproduce the correct QCD flavour anomaly in the ENJL-like models effective action we are working with, lead to the use of the following consistent one-loop anomalous Ward identity

$$\begin{aligned}
\partial_\mu A_{ii}^\mu(x) &= 2M_i P_{ii}(x) + \frac{N_c}{16\pi^2} \varepsilon_{\mu\nu\alpha\beta} \left(v_{ki}^{\mu\nu}(x) v_{ik}^{\alpha\beta}(x) \right. \\
&+ \frac{4}{3} d^\mu a_{ki}^\nu(x) d^\alpha a_{ik}^\beta(x) + \frac{2}{3} i \left\{ v_{ki}^{\mu\nu}(x), a_{im}^\alpha a_{mk}^\beta(x) \right\} \\
&+ \left. \frac{8}{3} i (a^\alpha v^{\mu\nu} a^\beta)_{ii}(x) + \frac{4}{3} (a^\mu a^\nu a^\alpha a^\beta)_{ii}(x) \right)
\end{aligned}$$

with

$$\begin{aligned}
v^{\mu\nu} &\equiv \partial^\mu v^\nu - \partial^\nu v^\mu - i [v^\mu, v^\nu] \quad \text{and} \\
d^\mu a^\nu &\equiv \partial^\mu a^\nu - i [v^\mu, a^\nu].
\end{aligned} \tag{4.24}$$

Where v^μ and a^μ are the external vector and axial-vector sources defined in eq. (2.1). As shown in ref. [9], when using this Ward identity, the fact that the anomalous part in eq. (4.24) only contains external fields amounts to keeping the usual Wess-Zumino term [24] (the only one of $\mathcal{O}(p^4)$ in the chiral counting) for couplings of pseudoscalar type via G_S to external fields but when there are couplings to spin-1 fields via the G_V term, only the local chiral invariant part of the full term remains. We have checked that the form of the action given in [9] yields the same result as the one given below.

So when we use the one-loop anomalous Ward identity in eq. (4.24) to reduce the right-hand side of Tail I to a part with only pseudoscalar couplings to the one-loop vertex, we obtain a local chiral invariant result plus an extra part where Tail I couples directly to the external vector sources $v_\mu^{kl}(x) v_\nu^{mn}(y)$. This extra part is of order p^4 and is the subtraction the anomalous Ward identity imposes to obtain the correct QCD flavour anomaly.

The full result in terms of the one-loop $\overline{\Pi}_{\mu\nu}^+$ three-point function is given by

$$\begin{aligned}
\Pi_{\mu\nu}^+(p_1, p_2) &= \overline{\Pi}_{\mu\nu}^+(p_1, p_2) \left(\frac{M_V^2(-p_1^2)_{ii} M_V^2(-p_2^2)_{ii}}{(M_V^2(-p_1^2)_{ii} - p_1^2) (M_V^2(-p_2^2)_{ii} - p_2^2)} \right) \\
&\times \left\{ 1 + \frac{4\pi^2 G_S}{N_c \Lambda_\chi^2} \Pi_P(-q) - \frac{8\pi^2 G_V}{N_c \Lambda_\chi^2} 2M_i \Pi_P^M(-q) \right\} \\
&+ \overline{\Pi}_{\mu\nu}^+(p_1, p_2) \Big|_{p_1^2=p_2^2=q^2=0} \frac{8\pi^2 G_V}{N_c \Lambda_\chi^2} 2M_i \Pi_P^M(-q). \tag{4.25}
\end{aligned}$$

Where the one-constituent quark loop function $\overline{\Pi}_{\mu\nu}^+$ is given by

$$\begin{aligned} \overline{\Pi}_{\mu\nu}^+(p_1, p_2) &= \frac{N_c}{16\pi^2} \varepsilon_{\mu\nu\beta\rho} p_1^\beta p_2^\rho F(p_1^2, p_2^2, q^2) \frac{2}{M_i} \\ \text{with } F(p_1^2, p_2^2, q^2) &= 1 + I_3(p_1^2, p_2^2, q^2) - I_3(0, 0, 0) \end{aligned} \quad (4.26)$$

where the form factor $I_3(p_1^2, p_2^2, q^2)$ is the one given in appendix D and which appeared before in the study of the VPP three-point function in section (4.1). This form factor coincides with the one found in the context of constituent quark-models (see for instance [25]) when the cut-off Λ_χ is sent to ∞ . Here, this is a physical scale of the order of the spontaneous symmetry breaking scale and therefore we have to keep it finite. The anomalous Ward identities in eq. (4.24) is telling us that terms which are of chiral counting different to $\mathcal{O}(p^4)$ have to be local chiral invariant [9] but they do not fix the regularization for those terms. We therefore use here consistently the same regularization for them as in the non-anomalous sector. At $\mathcal{O}(p^4)$ the chiral anomaly also uniquely fixes the one-loop constituent chiral quark anomalous form factor to be the one in eq. (4.26) when $p_1^2 = p_2^2 = q^2 = 0$ [26].

Here we have used the anomalous Ward identity in eq. (4.22). A naive use of the two-point functions and Ward identities would have led only to the first term in the sum in eq. (4.25). The second term is the result of enforcing the validity of the QCD flavour anomaly. Substituting the results on the two-point functions in section 3 we can write down the following explicit expression

$$\begin{aligned} \Pi_{\mu\nu}^+(p_1, p_2) &= \frac{N_c}{16\pi^2} \varepsilon_{\mu\nu\beta\rho} p_1^\beta p_2^\rho \left(\frac{4M_i}{g_S f_{ii}^2(-q^2) (m_{ii}^2(-q^2) - q^2)} \right) \\ &\left\{ 1 - g_A(-q^2)_{ii} \left[1 - F(p_1^2, p_2^2, q^2) \frac{M_V^2(-p_1^2)_{ii} M_V^2(-p_2^2)_{ii}}{(M_V^2(-p_1^2)_{ii} - p_1^2) (M_V^2(-p_2^2)_{ii} - p_2^2)} \right] \right\}. \end{aligned} \quad (4.27)$$

We refer to section 5.3 for the definition of the physical anomalous $\pi^0 \gamma^* \gamma^*$ form factor after reducing this PVV three-point function. We shall also discuss there on the VMD limit in this process and give some numerics.

5 Meson-Dominance

5.1 Two-point functions

Here we shall discuss the vector case, the axial-vector case is similar. The transverse vector two-point function in eq. (3.34) reduces in the diagonal case, $m_i = m_j$ (the off-diagonal case can be done analogously) to the following simple expression

$$\Pi_V^{(1)}(-q^2) = 2f_V^2(-q^2) \frac{M_V^2(-q^2)}{M_V^2(-q^2) - q^2} \quad (5.1)$$

$$\text{with } 2f_V^2(-q^2)M_V^2(-q^2) = \frac{N_c\Lambda_\chi^2}{8\pi^2G_V} \quad (5.2)$$

$$\text{and } 2f_V^2(-q^2) = \overline{\Pi}_V^{(1)}(-q^2). \quad (5.3)$$

In the complete VMD limit this two-point function has the same form but with f_V and M_V constants. Let us see how complete VMD works in this model. For that, we shall study the inverse of $\Pi_V^{(1)}(-q^2)$, which in the complete VMD limit is a straight line. This function was plotted in section 3.9 in figure 3. There we can see that $\Pi_V^{(1)}(-q^2)$ in this model is very near of reproducing the complete VMD linear form. Moreover, we can perform a linear fit to the inverse of $\Pi_V^{(1)}(-q^2)$ to obtain the best VMD values for the f_V and M_V parameters. These parameters are in this way meaningfully defined in the Euclidean region $-q^2 > 0$ where the model is far from the two constituent quark threshold. Doing this type of fit for the values of the input parameters Λ_χ , G_V , G_S discussed in section 3.9 leads to $M_V \simeq 0.644$ GeV for the vector mass in the chiral limit (remember that we are always in the large N_c limit) and $f_V \simeq 0.17$ for the decay constant. For current quark masses values discussed also in section 3.9, we obtain for the ρ meson flavour configuration $M_\rho \simeq 0.655$ GeV and $f_\rho \simeq 0.17$ and for the ϕ meson one $M_\phi \simeq 0.790$ GeV and $f_\phi \simeq 0.14$. We see thus that the ρ mass is very close in the large N_c limit, to the one in the chiral limit, M_V . Notice that these values for M_V are far away from those quoted in ref. [4]. The underlying reason is that in ref. [4] f_V and M_V were determined directly from the Lagrangian at $\mathcal{O}(p^2)$ in the ENJL expansion, identifying them with their values at $q^2 = 0$. What we find here is that even though the two-point function in eq. (5.1) has the correct $q^2 \rightarrow 0$ limit behaviour it does have, with the choice of vector fields to represent vector particles in ref. [4], substantial contributions from higher order terms (mainly of $\mathcal{O}(p^4)$ in the ENJL expansion). A physical vector field that would include these contributions can in principle be defined as is shown by the fact that the inverse of $\Pi_V^{(1)}(-q^2)$ is a rather straight line. What has happened is that

$$\Pi_V^{(1)}(-q^2) \simeq \frac{\left(2f_V^2M_V^2\right)_{q^2=0}}{M_V^2(0) - q^2 \left(1 + \lambda + \mathcal{O}(q^2/\Lambda_\chi^2)\right)}. \quad (5.4)$$

The vector meson mass derived in [4] was $M_V(0)$ while the slope of the physical two-point function (for $|q^2|/\Lambda_\chi^2 \ll 1$ that is where this ENJL cut-off model makes sense) corresponds to rather $M_V \sim M_V(0)/\sqrt{1 + \lambda}$. We find from the calculation that indeed λ is of order 1 ($\lambda \simeq 0.7$), explaining the difference in the slope from the $\mathcal{O}(p^2)$ ENJL calculation in ref. [4] of the two-point function to the $\mathcal{O}(p^4)$ one.

We can also see from eqs. (3.39), (3.51)-(3.53) and (3.60) that the forms of these two-point functions are very similar to the corresponding ones in the meson dominance limit but with couplings varying with q^2 . The identification of the corresponding physical values will involve analogous procedures to the one described above for the transverse vector two-point function one.

5.2 VPP three-point function

In this subsection we discuss how the result for the three-point function $\Pi_\mu^{VPP}(p_1, p_2)$ obtained in section 4.1 can be used to determine the physical pion electromagnetic form factor in this model. We shall discuss the VPP three-point function flavour structure corresponding to the three-point function $\Pi_\mu^+(p_1, p_2)$ in eq. (4.17) for $m \equiv m_i = m_j = m_k$ and $p^2 \equiv p_1^2 = p_2^2$ for definiteness.

Since this $\Pi_\mu^+(p_1, p_2)$ is a Green's function we first have to reduce the external legs to properly normalized pion fields. The vector leg acts here as an external source and is properly reduced without bringing in any factor. For this, we first look at the pseudoscalar two-point function in eq. (3.53) obtained using the same external fields and parametrize it around the pole as

$$\Pi_P(-p^2) = -\frac{1}{g_S} + \frac{Z_\pi}{p^2 - m_\pi^2} \left(1 + \mathcal{O}(m_\pi^2/\Lambda_\chi^2)\right). \quad (5.5)$$

The reducing factor Z_π is

$$\begin{aligned} Z_\pi &\equiv -\frac{(M_i + M_j)^2}{2f_\pi^2(-m_\pi^2)g_S^2} \frac{1}{A^2} && \text{with} \\ A^2 &= 1 - \left. \frac{\partial m_{ij}^2(-p^2)}{\partial p^2} \right|_{p^2=m_\pi^2} \\ &= 1 + \frac{g_A^2(-m_\pi^2)}{2f_\pi^2(-m_\pi^2)} \left[\bar{f}_\pi^2(0) - \bar{f}_\pi^2(-m_\pi^2) + 2m_\pi^2 I_3(m_\pi^2, m_\pi^2, 0) \right] \end{aligned} \quad (5.6)$$

where $I_3(p_1^2, p_2^2, q^2)$ defined in appendix D and $f_\pi^2(-q^2)$ and $\bar{f}_\pi^2(-q^2)$ in eqs. (3.40)-(3.41). The quantity A is very close to one and exactly one in the chiral limit. Each pion leg brings a factor $Z_\pi^{1/2}$ after reducing the Green's function to the physical amplitude. Rewriting the pseudoscalar two-point function in the form in eq. (5.5) gives that m_π^2 is the solution of $m_\pi^2 = m_{ij}^2(-m_\pi^2)$.

Reducing the VPP three-point function $\Pi_\mu^+(p_1, p_2)$ in eq. (4.17) we find that it can be written as follows² (we shall suppress the flavour indices which are always *ii*)

$$\Pi^{+\mu}(p_1, p_2) = \frac{Z_\pi}{(p^2 - m_\pi^2)^2} F_{VPP}(p^2, q^2) (p_2 - p_1)^\mu \quad (5.7)$$

which defines the electromagnetic pion form factor (or in general the pseudoscalar vector form factor) $F_{VPP}(p^2, q^2)$ in this model. (The general pion form factor, i.e different quark masses and $p_1^2 \neq p_2^2$ can be obtained similarly from (4.17).) This form factor in the ENJL model is expected to be a good approximation

²To obtain the $\gamma^* \pi^+ \pi^-$ three-point function from this Π_μ^+ is necessary to multiply it by the electric charge of the pion.

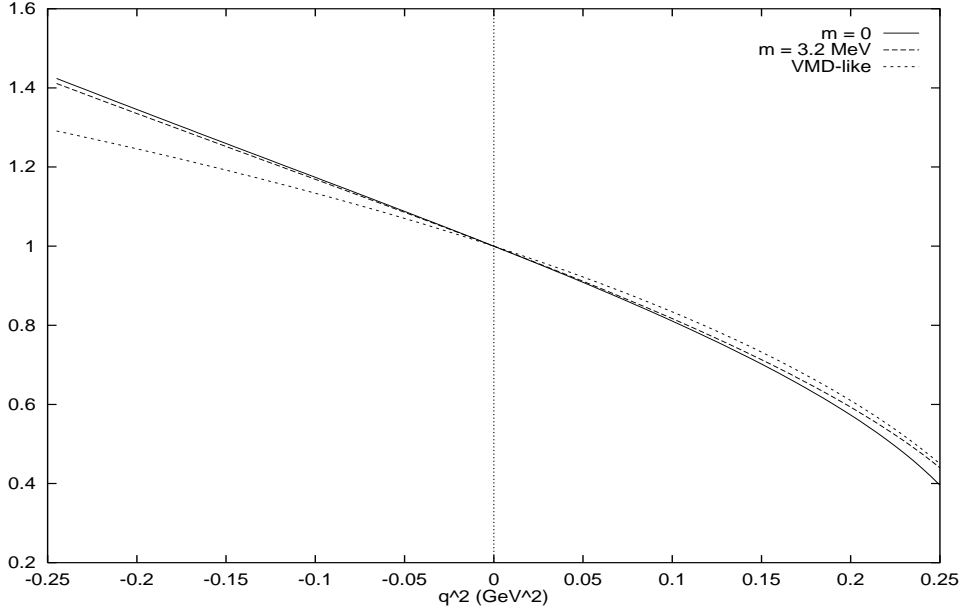


Figure 8: The inverse of the vector form factor of the pion of eq. (5.8). For the chiral limit and with all current quark masses equal to 3.2 MeV. Also plotted is the VMD approximation $M_V^2(-q^2)/(M_V^2(-q^2) - q^2)$ for the latter case.

at intermediate and low-energy energies, within the validity of the ENJL model we are working with, i.e. for $|q^2| \ll \Lambda_\chi^2$. The explicit expression for this form factor³ is

$$\begin{aligned}
F_{VPP}(m_\pi^2, q^2) &= \frac{1}{2A^2 f_\pi^2(-m_\pi^2)} \frac{M_V^2(-q^2)}{M_V^2(q^2) - q^2} \left\{ 2f_\pi^2(-m_\pi^2) \right. \\
&- q^2(1 - g_A(-m_\pi^2))^2 f_V^2(-q^2) + \frac{2g_A^2(-m_\pi^2)}{q^2 - 4m_\pi^2} \\
&\times \left. \left[(q^2 - 2m_\pi^2)(\bar{f}_\pi^2(-q^2) - \bar{f}_\pi^2(-m_\pi^2)) - 4m_\pi^4 I_3(m_\pi^2, m_\pi^2, q^2) \right] \right\}.
\end{aligned} \tag{5.8}$$

Notice that this form factor has no pole at $q^2 = 4m_\pi^2$. The value of A^2 in eq. (5.6) is precisely the one that ensures that $F_{VPP}(m_\pi^2, 0) = 1$ in the large N_c limit as is required by the electromagnetic gauge invariance. This must be so since we have imposed the Ward identities to obtain this form factor. In figure 8 we have plotted the inverse of this form factor for the parameters quoted in section 3.9 in the chiral case ($\bar{m} = 0$) and in the case corresponding to the physical pion mass ($\bar{m} = 3.2$ MeV). As can be seen from the picture, it is a rather straight line so

³This form factor was also calculated in ref. [8]. With the appropriate changes of notation it agrees with the one found there.

the complete VMD result for this form factor, i.e.,

$$F_{VPP}^{VMD}(m_\pi^2, q^2) = \frac{M_\rho^2}{M_\rho^2 - q^2} \quad (5.9)$$

with constant vector mass M_ρ works rather well. The slope of the linear fit of the inverse of the form factor in eq. (5.8) to this VMD form gives a vector mass which is $M_\rho \simeq 0.77$ GeV. This mass is very close to the physical value and rather different from the one found for the transverse vector two-point function in the VMD limit $M_\rho \simeq 0.655$ GeV in the large N_c limit. This explains why using the physical ρ meson mass and the VMD dominance works so well but it also shows that this M_ρ “mass” in eq. (5.9) has not, in principle, to be the same as the mass of the vector meson described by the transverse two-point vector function.

The same three-point function VPP also contains implicitly the $\rho \rightarrow \pi\pi$ coupling constant g_V . (See ref. [4] for its definition. Notice that is different from the symbol used in section 3.) Again, to obtain the physical $\rho \rightarrow \pi\pi$ amplitude we should first reduce the vector leg that now corresponds to the ρ particle, (remember that the pion legs have been already reduced). This will bring a factor which is similar to the factor $1 + \lambda$ discussed in the previous subsection. We shall, as before, first determine the reducing vector factor from the vector two-point function in eq. (5.1). The reducing factor Z_ρ is

$$\begin{aligned} Z_\rho &\equiv -\left(2f_V^2 M_V^2\right) \left(1 - \frac{\partial M_V^2(-q^2)}{\partial q^2} \Big|_{q^2=M_\rho^2}\right)^{-1} \\ &\equiv -\frac{2f_V^2 M_V^2}{B^2}. \end{aligned} \quad (5.10)$$

In this equation the combination $2f_V^2 M_V^2$ is the one given in eq. (5.2) and is independent of q^2 . The vector mass M_ρ is again given by the solution to $M_\rho^2 = M_V^2(-M_\rho^2)$.

One also can rewrite down the electromagnetic pion form factor showing explicitly the coupling constant of the ρ meson to pions, g_V , as follows

$$F_{VPP} = 1 + f_V g_V \frac{q^2}{f_\pi^2} \frac{M_\rho^2}{M_\rho^2 - q^2}. \quad (5.11)$$

Then, in the complete VMD limit one has $f_V g_V = f_\pi^2/M_\rho^2$. In this ENJL model this relation is equivalent to $g_V = (1 - g_A)f_V$, i.e. one has complete VMD and the KSRF relation [11] $2g_V = f_V$ satisfied for $g_A = 1/2$.

One can see in the eq. (5.11), that reducing the ρ vector leg brings in a factor B^2 in the numerator and another factor B^2 in the denominator with the net result that $f_V(-q^2)g_V(-q^2)$ is not affected by reducing of the vector leg as

much as happens to $f_V^2(-q^2)$ in eq. (5.1). Then, with the definition of $f_V g_V$ in eq. (5.11) we get the following

$$\begin{aligned}
& f_V(-q^2)g_V(-q^2) \equiv \\
& \frac{1}{2A^2q^2} \left[(q^2 - M_V^2(-q^2)) \left(2A^2 f_\pi^2(-m_\pi^2)/M_V^2(-q^2) - f_V^2(-q^2)(1 - g_A(-m_\pi^2))^2 \right) \right. \\
& + (1 + g_A(-m_\pi^2))f_\pi^2(-m_\pi^2) + \frac{2g_A^2(-m_\pi^2)}{q^2 - 4m_\pi^2} \\
& \left. \times \left((q^2 - 2m_\pi^2)(\bar{f}_\pi^2(-q^2) - \bar{f}_\pi^2(-m_\pi^2)) - 4m_\pi^4 I_3(m_\pi^2, m_\pi^2, q^2) \right) \right].
\end{aligned} \tag{5.12}$$

Notice that this $f_V(-q^2)g_V(-q^2)$ form factor has neither a pole at $q^2 = 0$ nor at $q^2 = 4m_\pi^2$ and when expanded in q^2 and with $m_\pi^2 = 0$ one gets $f_V(0)g_V(0) = 2L_9$, where L_9 is the one found in ENJL in ref. [4]. As discussed there, at $q^2 = 0$ one has the KSRF [11] relation, i.e. $f_V(0) = 2g_V(0)$ (which is valid for $q^2 = m_\pi^2 = 0$) analytically for $g_A = 0$ and very approximately satisfied for g_A varying between 0 and 1. The expression in eq. (5.12) is the off-shell equivalent to the KSRF relation in this model. For $g_A = 0$ the vector mass vanishes and the ρ meson couples as an $SU(3)_V$ gauge boson, in fact in this limit one recovers the results of the Hidden Gauge Symmetry model [27] for the non-anomalous sector. In particular, when $g_A = 0$ we have that the reducing factor B is 1 as corresponds to external gauge sources. In this limit ($g_A = 0$), one still has the KSRF relation analytically satisfied off-shell, i.e. $f_V(-q^2) = 2g_V(-q^2)$ for all q^2 .

In the limit $g_A \rightarrow 1$ one has

$$\begin{aligned}
& f_V(-q^2)g_V(-q^2) \rightarrow \frac{1}{A^2q^2} \left[f_\pi^2(-m_\pi^2)(1 - A^2) + \frac{1}{q^2 - 4m_\pi^2} \right. \\
& \left. \times \left((q^2 - 2m_\pi^2)(f_\pi^2(-q^2) - f_\pi^2(-m_\pi^2)) - 4m_\pi^4 I_3(m_\pi^2, m_\pi^2, q^2) \right) \right].
\end{aligned} \tag{5.13}$$

This is the constituent quark model result (in $g_A = 1$ the vector mesons decouple from this model) and when expanded in q^2 with $m_\pi^2 = 0$ it coincides with the corresponding result in ref. [4]. The KSRF relation is not analytically fulfilled in this limit but one can see that analytically is very approximately satisfied. Then, we have that for g_A varying between 0 (the gauge vector limit) and 1 (the constituent quark limit) the KSRF relation goes from being analytically fulfilled to be very approximately fulfilled for any value of q^2 .

Let us see how $g_V(-q^2)$ works numerically compared with $f_V(-q^2)$ for a definite value of g_A . In figure 9 we plot $f_V(-q^2)/2$ and $g_V(-q^2)$ for the values of parameters discussed in section 3.9. These values correspond to $g_A(0) = 0.61$. The form factor $g_V(-q^2)$ is somewhat dependent on q^2 with $(2.1 \sim 2.2) g_V(-q^2) \simeq f_V(-q^2)$ in the Euclidean region. In this figure we also plot the case $g_A \rightarrow 1$ where the same features can be seen. The form factor $g_V(-q^2)$ for any value of g_A will be between the line $f_V/2$ (i.e., the $g_A = 0$ limit) and the line for $g_A = 1$, therefore the KSRF relation is approximately satisfied off-shell for any value of g_A .

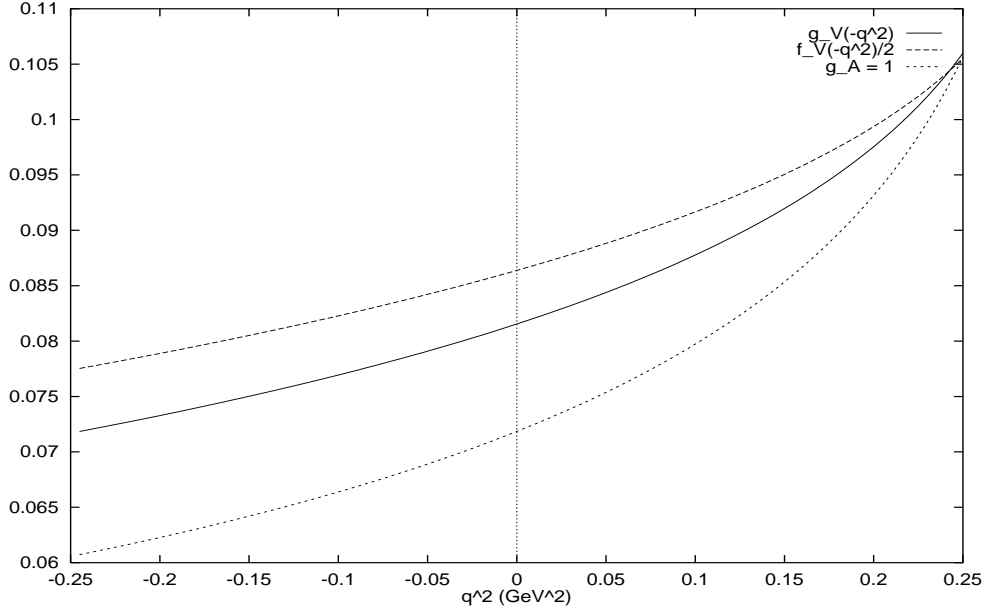


Figure 9: The generalized KSRF relation. We plot $g_V(-q^2)$ for $g_A = 0.61$ (solid line); $g_A \rightarrow 1$ (short-dashed line) and $f_V(-q^2)/2$ (dashed line). The difference between the curves gives the violation of the KSRF relation. See text for further comments.

5.3 PVV three-point function

In this subsection we want to study the $\pi^0 \gamma^* \gamma^*$ anomalous form factor. For that we shall reduce the PVV Green's function in eq. (4.27) calculated in section 4.2 to the physical amplitude following the same procedure that in the previous section (for details see there). Now, we have to reduce one pion leg, this will bring in a factor $\sqrt{Z_\pi}$ and two external vector sources legs which are properly reduced without bringing any factor. Then the PVV three-point function in eq. (4.27)⁴ can be rewritten as follows

$$\begin{aligned} \Pi_{\mu\nu}^+(p_1, p_2) &= \frac{\sqrt{Z_\pi}}{q^2 - m_\pi^2} \frac{N_c}{16\pi^2} i\varepsilon_{\mu\nu\beta\rho} p_1^\beta p_2^\rho \frac{2\sqrt{2}}{f_\pi(-m_\pi^2)} \\ &\times F_{PVV}(q^2, p_1^2, p_2^2) \end{aligned} \quad (5.14)$$

where F_{PVV} is the $\pi^0 \rightarrow \gamma^* \gamma^*$ form factor in this model. Notice that the reducing factor A in eq. (5.6) goes to one in the chiral limit preserving, in that way, the chiral anomaly condition $F_{PVV}(0, 0, 0) = 1$. This form factor can be used as an accurate interpolating expression in low-energy hadronic processes valid for

⁴To obtain the $\pi^0 \gamma^* \gamma^*$ three-point function from this $\Pi_{\mu\nu}^+$ is necessary to multiply it by a factor $\sqrt{2}$ coming from the π^0 flavour structure and a factor $e^2/3$ from the quarks electric charge.

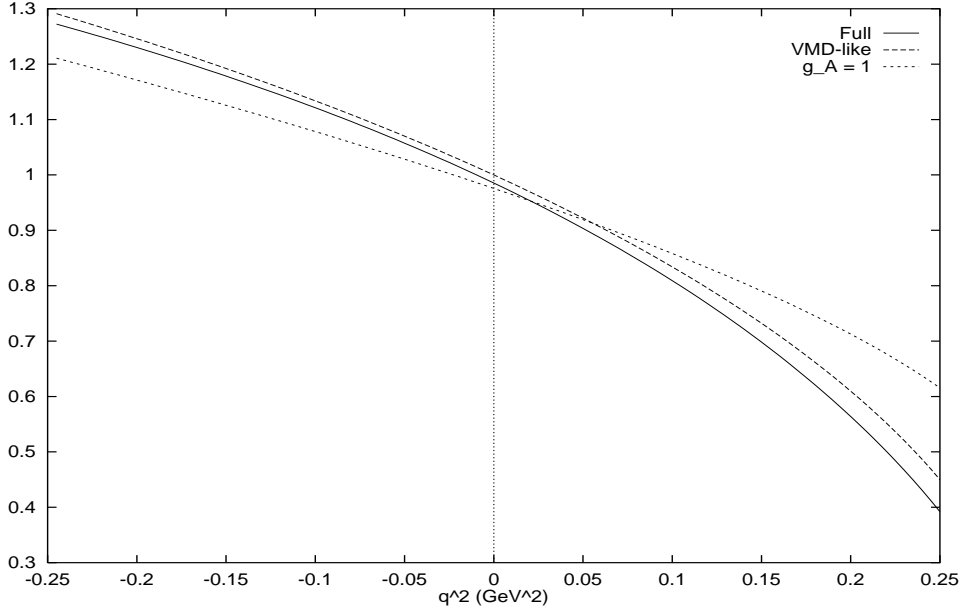


Figure 10: The inverse of the $\pi^0\gamma^*\gamma$ form factor for one photon on-shell and one off-shell as a function of the photon mass squared, q^2 . Notice the linearity in the Euclidean region. Plotted are the full result, $M_V^2(-q^2)/(M_V^2(-q^2) - q^2)$ (VMD-like) and the ENJL model without vector and axial-vector mesons ($g_A = 1$).

external momenta smaller than Λ_χ^2 . We plot the inverse of this form factor for the case $p_2^2 = 0$ in figure 10. Notice that there $F_{PVV}(m_\pi^2, 0, 0) \neq 1$ and the difference comes from the reducing factor A and is of chiral counting $\mathcal{O}(p^6)$. We can expand this form factor for small p_1^2, p_2^2 and pion mass⁵ as follows

$$F_{PVV}(m_\pi^2, p_1^2, p_2^2) = 1 + \rho(p_1^2 + p_2^2) + \rho' m_\pi^2 + \mathcal{O}(q^4), \quad (5.15)$$

this expansion defines the slopes ρ and ρ' which in this model are

$$\begin{aligned} \rho &= g_A(0) \left(\frac{1}{M_V^2(0)} + \frac{\Gamma(2, M^2/\Lambda_\chi^2)}{12M^2} \right), \\ \text{and } \rho' &= g_A(0) \left(\frac{\Gamma(2, M^2/\Lambda_\chi^2)}{12M^2} - \frac{\Gamma(1, M^2/\Lambda_\chi^2)}{12\Gamma(0, M^2/\Lambda_\chi^2)M^2} \right). \end{aligned} \quad (5.16)$$

Where the second term in ρ' comes from the reducing factor A defined. The constituent quark mass M here is the one corresponding to the current quark mass value $\bar{m} = 3.2$ MeV used in the numerical applications section 3.9. Using $M_V^2(0) = 6M^2 g_A(0)/(1 - g_A(0))$ [4] we can write down them as

$$\rho = \frac{1}{12M^2} \left(2 - \left(2 - \Gamma(2, M^2/\Lambda_\chi^2) \right) g_A(0) \right)$$

⁵For the π^0 decay we are on the pole and hence $q^2 = m_\pi^2$

and

$$\rho' = \frac{g_A(0)}{12M^2} \left(\Gamma(2, M^2/\Lambda_\chi^2) - \frac{\Gamma(1, M^2/\Lambda_\chi^2)}{\Gamma(0, M^2/\Lambda_\chi^2)} \right) \quad (5.17)$$

which interpolate between the constituent quark-model result $g_A(0) = 1$ and the gauge vector meson result $g_A(0) = 0$.

With the input parameters we have been using (see numerical application section 3.9) we get

$$\begin{aligned} \rho &= (0.86 + 0.67) = 1.53 \text{ GeV}^{-2} \\ \text{and} \quad \rho' &= (0.67 - 0.27) = 0.40 \text{ GeV}^{-2}. \end{aligned} \quad (5.18)$$

Where for ρ the first number between brackets is the vector meson exchange contribution and the second is the constituent quark contribution (up to $g_A(0)$). We see that both contributions are very similar giving some kind of complementarity between both approaches and explaining the relative success of both when used to describe this slope. For ρ' they are the constituent quark contribution and the one coming from the pion leg reducing factor $1/A$. (Notice the cancellation there.)

In the limits $g_A \rightarrow 1$ and $g_A \rightarrow 0$ we find

$$\begin{aligned} \rho &= 1.10 \text{ GeV}^{-2} \quad \text{for } g_A \rightarrow 1, \\ \rho &= 2.20 \text{ GeV}^{-2} \quad \text{for } g_A \rightarrow 0, \\ \rho' &= 0.66 \text{ GeV}^{-2} \quad \text{for } g_A \rightarrow 1, \\ \text{and} \quad \rho' &= 0.00 \text{ GeV}^{-2} \quad \text{for } g_A \rightarrow 0. \end{aligned} \quad (5.19)$$

We see that the difference between these two limits is big and that the actual result is some kind of interpolation. Experimentally [28]

$$\rho = (1.8 \pm 0.14) \text{ GeV}^{-2}. \quad (5.20)$$

Taking into account that the $1/N_c$ corrections from χ PT loops are estimated [29] to be twice the experimental error we consider the result as good.

Let us compare this full result in eq. (5.17) with the one obtained in ref. [30] in this same model assuming complete VMD in the chiral limit. There, the same prescription to include the QCD chiral anomaly that here [9] was used at the one-loop level with the result

$$\rho = \frac{1}{12M^2} \frac{1 - g_A^2(0)}{g_A(0)}. \quad (5.21)$$

Of course, this complete VMD result vanishes when $g_A = 1$ where vector mesons decouple. The differences between eq. (5.17) and eq. (5.21) come from the resummation of all the orders in external momenta that are included in the full result in eq. (5.17). One can see that the complete VMD result coincides with the full result for $g_A(0) \simeq 0.50$.

6 Conclusions

In this paper we have derived in a general class of ENJL-like models the two-point functions away for the chiral limit and for different masses in terms of the one-loop ones. This derivation used the Ward identities of the one-loop functions. The heat kernel expansion yields two more identities than can be derived from the current identities directly. These are then used to rewrite all two-point functions in terms of two basic ones. These can then be calculated in the bare ENJL-model as we did here or gluonic background corrections can be taken into account (see ref. [5] for a discussion). These extra identities allow us to discuss the Weinberg Sum Rules in this class of models. We find that the first WSR is satisfied and the third one is broken in the same way as required in QCD. The second WSR is satisfied in this model while QCD requires it to be broken. The very high energy behaviour is thus a little too suppressed.

We also find (in the case of equal masses) the simple formula for the scalar mass that had been argued before when only divergent terms were kept in the heat kernel expansion (see second paper in ref. [2]). All two-point functions can also be written in a form very like a form of meson dominance but with the couplings and masses depending on the momentum. In the Euclidean region, $q^2 \leq 0$, the vector two-point function can also be well described by a VMD form with constant couplings. The relation of these with those from the low-energy expansion was treated as well.

We then proceeded to calculate two examples of three-point functions. Again the use of Ward identities simplified the calculation and pinpoints all the regularization ambiguities into the one-loop function. We want to point out that both the anomalous sector and the non-anomalous sectors of these ENJL-like models are then treated on the same foot and VMD can be discussed in both sectors with a unique prescription, namely the use of the relevant Ward identities [5, 9]. Then the regularization dependence uncertainties are consistently treated within the same prescription in both the anomalous sector and the non-anomalous sector. Here we discussed Vector Meson Dominance and the KSRF relation for the VPP case. We then use the Ward identities, modified to reproduce the QCD flavour anomaly, to calculate the PVV function. Here we find that naive VMD expectations for this function cannot be realized. No simple generalization to q^2 dependent couplings is possible. Formally our expression looks very much like the VMD expression with couplings and vector mass running with q^2 times $g_A(-q^2)$ plus a second term coming from the requirements of the anomaly. The numerical result for the slope is, however, in good agreement with the VMD value. But the $g_A(-q^2)$ factor diminished the “real” VMD part to a little more than half the full value while the constituent quark loop adds the remainder. Here we reconcile both explanations for the slope, the VMD one and the quark loop one, [25, 29].

Acknowledgements

We would like to thank E. de Rafael for encouragement. The work of JP has been supported in part by CICYT (Spain) under Grant Nr. AEN93-0234.

A Proper time and incomplete Gamma functions

In this appendix we give the regularization method we have used throughout this work and some related definitions. After performing the standard Feynman parametrization, one constituent fermion propagator is regulated consistently in this work using a proper time regulator as follows

$$\frac{1}{M^2(Q^2, x)} \Rightarrow \int_{1/\Lambda_\chi^2}^{\infty} d\tau e^{-\tau M^2(Q^2, x)}. \quad (\text{A.1})$$

After performing the remaining Q^2 integration and the change of variables $\tau\Lambda_\chi^2 \rightarrow z$ one arrives to the following type of integrals

$$\Gamma(n-2, \epsilon) = \int_{\epsilon}^{\infty} \frac{dz}{z} z^{n-2} e^{-z}, \quad (\text{A.2})$$

with $\epsilon \equiv M^2(Q^2, x)/\Lambda_\chi^2$ and $n = 1, 2, \dots$. These $\Gamma(m, y)$ are the so-called incomplete Gamma functions.

In general, this regulator breaks the Ward identities. We have, however, always imposed all the Ward identities explicitly so our results have the correct symmetry covariance.

B Derivation of the Ward identities

In this appendix we generalize the proof in the appendix of ref. [5] to the case with nonzero current quark masses. There a proof was given of all relevant identities in terms of the heat kernel expansion (for an excellent recent review and definitions see ref. [31]) and some of them in terms of the Ward identities as well. Here those which can be derived directly from the Ward identities can also be derived from the heat kernel expansion but since they involve different masses they require a resummation of different terms. For these the direct derivation of the Ward identities is actually simpler. Only for the additional relations will we give the heat kernel derivation.

At the one-loop level we use as Lagrangian the one in eq. (2.2) (with the same definitions as there)

$$\mathcal{L}_{\text{ENJL}} = \bar{q}\mathcal{D}q \quad (\text{B.1})$$

where \mathcal{D} contains the couplings to the external fields l_μ, r_μ, s and p as well as the effects of the four-quark terms in $\mathcal{L}_{\text{NJL}}^{\text{S,P}}$ and $\mathcal{L}_{\text{NJL}}^{\text{V,A}}$ on the quark currents at the one-loop level. In particular it contains the constituent quark masses, M_i . However, we shall keep the notation l_μ, r_μ, s and p to denote the quark current sources in the presence of these four-quark NJL operators. The one-loop current identities derived from this Lagrangian are

$$\begin{aligned}\partial^\mu V_\mu^{ij} &= -i(M_i - M_j) S^{ij} \\ \partial^\mu A_\mu^{ij} &= (M_i + M_j) P^{ij} .\end{aligned}\tag{B.2}$$

When the whole series of constituent quark bubbles are summed these identities are satisfied changing constituent quark masses by current quark masses. In addition we use the equal time commutation relations for fermions

$$\left\{ q_\alpha^{i\dagger}(x), q_\beta^j(y) \right\}_{x^0=y^0} = i\delta_{\alpha\beta}\delta_{ij}\delta^3(\mathbf{x} - \mathbf{y}) .\tag{B.3}$$

Here α and β are Dirac indices and \mathbf{x} means the spatial components of x . Multiplying the two-point functions with iq_μ is equivalent to taking a derivative of the exponential under the integrals in eqs. (3.5) to (3.8). By partial integration we then get several terms, those due to the time ordering which leads to equal time commutators and those where the derivative hits one of the currents. The first type are evaluated using eq. (B.3) and the second type are related to other two-point functions using eq. (B.2). This then leads to the expressions (3.26) to (3.27).

The derivation of the other two identities is slightly more complicated. The effective action of the Lagrangian in eq. (B.1) can be obtained in Euclidean space as a heat kernel expansion (see ref. [31]). The coefficients of this expansion are the so-called Seeley-DeWit coefficients, they are constructed out of the two quantities E and $R_{\mu\nu}$. These are defined as

$$\begin{aligned}\mathcal{D}^\dagger \mathcal{D} &\equiv -\nabla_\mu \nabla^\mu + E + \overline{M}^2 , \\ R_{\mu\nu} &\equiv [\nabla_\mu, \nabla_\nu] , \\ \nabla_\mu \# &\equiv \partial_\mu \# - i[v_\mu, \#] - i[a_\mu \gamma_5, \#] .\end{aligned}\tag{B.4}$$

If in eq. (B.1) the Dirac operator \mathcal{D} contains couplings to gluons these should not be taken into account in eq. (B.4). The relevant heat kernel expansion in that case will have different coefficients depending on vacuum expectation values of gluonic operators, but will still be constructed out of the quantities in eq. (B.4) (depending now also on the gluon field). The quantity \overline{M} is the mass that is used in the heat kernel expansion. The operator \mathcal{D} is

$$i\gamma^\mu(\partial_\mu - iv_\mu - ia_\mu \gamma_5) - \mathcal{M} - s + ip\gamma_5 .\tag{B.5}$$

Here $\mathcal{M} = \text{diag}(m_u, m_d, m_s)$ is the current quark mass matrix and we allow for spontaneous chiral symmetry breaking solution $\langle 0|s(x)|0\rangle \neq 0$. For the terms relevant to two-point functions we have

$$R_{\mu\nu} = -i(v_{\mu\nu} + a_{\mu\nu}\gamma_5),$$

and

$$\begin{aligned} E &= -\frac{i}{2}\sigma^{\mu\nu}R_{\mu\nu} + i\gamma^\mu d_\mu(M + s + ip\gamma_5) \\ &- \gamma^\mu \{a_\mu\gamma_5, M + s - ip\gamma_5\} + \{M, s\} - i[M, p]\gamma_5 + s^2 + p^2 \\ &+ M^2 - \overline{M}^2, \end{aligned}$$

with

$$\begin{aligned} v^{\mu\nu} &\equiv \partial^\mu v^\nu - \partial^\nu v^\mu - i[v^\mu, v^\nu], \\ a^{\mu\nu} &\equiv \partial^\mu a^\nu - \partial^\nu a^\mu - i[a^\mu, a^\nu], \\ d^\mu \# &\equiv \partial^\mu \# - i[v^\mu, \#]. \end{aligned} \tag{B.6}$$

The main difference with ref. [5] is the occurrence of the last line in the expression for E in (B.6). We shall call this last line E_0 . In this equation, $M \equiv \text{diag}(M_u, M_d, M_s)$, the diagonal matrix of the constituent quark masses defined in eq. (2.3). Notice that the scalar field here has been shifted and we have now $\langle 0|s(x)|0\rangle = 0$ (though we use the same notation for it). When $G_S \rightarrow 0$ in eq. (2.3) then $\overline{M} \rightarrow 0$ and $M \rightarrow \mathcal{M}$. Let us now systematically go through all possible types of terms in the expansion. We shall not discuss the mixed two-point functions here since we only want to prove eqs. (3.30)-(3.31).

In the heat kernel expansion, those terms containing two factors $R_{\mu\nu}$ only contribute to the transverse parts, $\overline{\Pi}_{V,A}^{(1)}$ and in the same way. Their contributions hence obviously satisfy eqs. (3.30)-(3.31). Similarly, one factor $R_{\mu\nu}$ requires the presence of two covariant derivatives ∇_μ . By commuting derivatives (the extra terms only contribute to three and higher point functions) and partial integration these can be brought next to each other so they convert into a second factor $R_{\mu\nu}$. This brings us back to the previous case. Intervening E 's can only contribute via E_0 but these do not spoil the above argument. The first term in E , namely $\sigma_{\mu\nu}R^{\mu\nu}$, requires a 2nd $\sigma_{\mu\nu}R^{\mu\nu}$ because otherwise the trace over Dirac indices vanishes. These also behave like terms with two factors $R^{\mu\nu}$. Therefore, in the remainder we are only concerned with E without this first term.

E can also directly contribute to the scalar and pseudoscalar two-point function in the same way via $s^2 + p^2$. Extra factors E become again E_0 and extra derivatives also respect the relation (3.31). The most complicated case is where both fields come from a different E . This contributes in the form $E_0^n E E_0^m \partial^{2i} E$. These contribute to all form factors in the form $M_i^n M_j^m q^{2i}$ times the coefficients listed in Table 1. These coefficients obviously satisfy the relations (3.30)-(3.31). The last type of terms is where the external fields come out of a derivative. We do not consider the mixed case here, so both the fields have to come out of a deriva-

Function	Contribution
$\bar{\Pi}_S$	$-q^2 + (M_i + M_j)^2$
$\bar{\Pi}_P$	$-q^2 + (M_i - M_j)^2$
$\bar{\Pi}_A^{(0)}$	$(M_i + M_j)^2/q^2$
$\bar{\Pi}_A^{(1)}$	$-(M_i + M_j)^2/q^2$
$\bar{\Pi}_V^{(0)}$	$(M_i - M_j)^2/q^2$
$\bar{\Pi}_V^{(1)}$	$-(M_i - M_j)^2/q^2$

Table 1: The contribution of terms of the type E^{m+n+2} to the two-point functions.

tive due to the γ_μ that is necessarily present in the E that would be a candidate for the external field. So there are those where the external fields are contained in two factors ∇_μ . If the indices of these are different, then there need to be at least two extra derivatives present that will produce a $q_\mu q_\nu$. This contributes equally to $\bar{\Pi}_V^{(0)}$ and $\bar{\Pi}_A^{(0)}$. If the indices are equal, it will contribute proportional to $g_{\mu\nu}$ and thus to the vector and axial-vector equally with $\bar{\Pi}_{V,A}^{(0+1)} = 0$. This completes the proof of the identities (3.30)-(3.31).

Now it remains to prove that these contributions will never produce a pole in $\bar{\Pi}^{(0+1)}$ at $q^2 = 0$. Terms that contain two factors $R_{\mu\nu}$ contain two factors of momenta and hence do not. Terms with one factor $R_{\mu\nu}$ can be brought in the form with two so do not produce a pole either. From Table 1 there is no contribution from that type of terms to $\bar{\Pi}_{V,A}^{(0+1)}$. Then those with external fields from ∇_μ with different derivatives necessarily contain extra factors $q_\mu q_\nu$ so do not contribute to a possible pole at $q^2 = 0$ and the last type of terms does not contribute to $\bar{\Pi}_{V,A}^{(0+1)}$ as shown above. This completes the proof.

C Explicit expressions for the barred two-point functions

Here we shall give the one-constituent-quark-loop expression for the two-point functions defined in eqs. (3.5)-(3.10) in the presence of current quark masses. These two-point functions are denoted in the text as the $\bar{\Pi}$ ones. They fulfil the same Ward identities as the full-ones in eqs. (3.26)-(3.29) changing the current quark masses there by the constituent quark ones. In addition, they also satisfy the Ward identities in eqs. (3.30)-(3.31). Using these identities one can see that there are only two independent functions out of $\bar{\Pi}_V^{(1)}$, $\bar{\Pi}_V^{(0)}$, $\bar{\Pi}_A^{(1)}$, $\bar{\Pi}_A^{(0)}$, $\bar{\Pi}_S^M$, $\bar{\Pi}_P^M$, $\bar{\Pi}_S$ and $\bar{\Pi}_P$. We shall take $\bar{\Pi}_P^M$ and $\bar{\Pi}_V^{(1)} + \bar{\Pi}_V^{(0)}$ as these functions. The explicit expressions are

$$\left(\overline{\Pi}_V^{(1)} + \overline{\Pi}_V^{(0)}\right) (Q^2)_{ij} = \frac{N_c}{16\pi^2} 8 \int_0^1 dx x(1-x) \Gamma(0, x_{ij}), \quad (\text{C.1})$$

$$\overline{\Pi}_P^M (Q^2)_{ij} = \frac{N_c}{16\pi^2} 4 \int_0^1 dx (M_i x + M_j(1-x)) \Gamma(0, x_{ij}), \quad (\text{C.2})$$

where

$$x_{ij} \equiv \frac{M_i^2 x + M_j^2(1-x) + Q^2 x(1-x)}{\Lambda_\chi^2}. \quad (\text{C.3})$$

One can obtain all the others one-loop two-point functions in function of these two by using the Ward identities mentioned above. For instance, for the $\overline{\Pi}_V^{(0)}$ one gets

$$\begin{aligned} \overline{\Pi}_V^{(0)} (Q^2)_{ij} &= -\frac{(M_i - M_j)^2}{M_i + M_j} \frac{\overline{\Pi}_P^M (Q^2)_{ij}}{Q^2(Q^2 + (M_i - M_j)^2)} \\ &\times \left\{ (M_i + M_j)^2 + g_A(Q^2)_{ij} m_{ij}^2(Q^2) \left(1 - \left(\frac{m_i - m_j}{m_i + m_j}\right) \left(\frac{M_i + M_j}{M_i - M_j}\right)\right) + Q^2 \right\}. \end{aligned} \quad (\text{C.4})$$

D Explicit expression for the one-loop form factor $\overline{\Pi}_\mu^+(p_1, p_2)$

Here we shall give the one-constituent-quark-loop expression for the three-point function $\overline{\Pi}_\mu^+(p_1, p_2)$ defined in eq. (4.3). We shall give it for $M_i = M_k = M_m$. The explicit expression is (remember that we have $j = m$),

$$\begin{aligned} \overline{\Pi}^{+\mu}(p_1, p_2) &= \\ &- \frac{1}{2M_i} \left\{ \overline{\Pi}_P^M(-p_1^2)_{ii} \right. \\ &+ \frac{p_1 \cdot p_2}{p_1^2 p_2^2 - (p_1 \cdot p_2)^2} \left[p_2^2 \left(\overline{\Pi}_P^M(-p_2^2)_{ii} - \overline{\Pi}_P^M(-q^2)_{ii} \right) \right. \\ &+ \left. (p_1 \cdot p_2) \left(\overline{\Pi}_P^M(-p_1^2)_{ii} - \overline{\Pi}_P^M(-q^2)_{ii} \right) \right] \\ &+ \left. \frac{2}{M_i} I_3(p_1^2, p_2^2, q^2) p_2^2 \left[1 + (p_1 \cdot p_2) \frac{p_1^2 + (p_1 \cdot p_2)}{p_1^2 p_2^2 - (p_1 \cdot p_2)^2} \right] \right\} p_1^\mu \\ &- (p_1 \leftrightarrow -p_2). \end{aligned} \quad (\text{D.1})$$

Where the two-point function $\overline{\Pi}_P^M(-p^2)$ was given in appendix C and the function $I_3(p_1^2, p_2^2, q^2)$ is

$$I_3(p_1^2, p_2^2, q^2) = \frac{N_c}{16\pi^2} 2M_i^2 \int_0^1 dx x \int_0^1 dy \frac{\Gamma(1, M^2(x, y)/\Lambda_\chi^2)}{M^2(x, y)} \quad (\text{D.2})$$

with

$$M^2(x, y) \equiv M_i^2 - p_1^2(1-x) - p_2^2x(1-y) + (p_1(1-x) - p_2x(1-y))^2. \quad (\text{D.3})$$

References

- [1] Y. Nambu and G. Jona-Lasinio, Phys. Rev. **122** (1961) 345, *ibid.* **124** (1961) 246
- [2] A. Dhar, R. Shankar and S.R. Wadia, Phys. Rev. **122** (1985) 3256 ;
D. Ebert and H. Reinhardt, Nucl. Phys. **B271** (1986) 188
- [3] T. Hatsuda and T. Kunihiro, QCD Phenomenology based on a Chiral Effective Lagrangian, Tsukuba preprint UTHEP-270 (to be published in Phys. Rep.) ;
Th. Meissner et al., Baryons in Effective Chiral Quark Models with Polarized Dirac Sea, report # RUB-TPII-42/93 (to be published in Rep. Prog. Theor. Phys.) ;
M.K. Volkov, Part. and Nuclei **24** (1993) 81 ;
W. Weise, Hadrons in the NJL model, (Lectures given at Center for Theoretical Physics, Seoul National Univ., Seoul, Korea; September 1992) Regensburg preprint TPR-93-2
- [4] J. Bijnens, C. Bruno and E. de Rafael, Nucl. Phys. **B390** (1993) 501
- [5] J. Bijnens, E. de Rafael and H. Zheng, Low-Energy Behaviour of Two-Point Functions of Quark Currents, CERN preprint CERN-TH.6924/93 (to be published in Z. Phys. C)
- [6] S. Klimt et al., Nucl. Phys. **A516** (1990) 429 ;
U. Vogl et al., Nucl. Phys. **A516** (1990) 469
- [7] M. Lutz and W. Weise, Nucl. Phys. **A518** (1990) 156

- [8] V. Bernard, U.-G. Meißner and A.A. Osipov, Phys. Lett. **B324** (1994) 201
- [9] J. Bijnens and J. Prades, Phys. Lett. **B320** (1994) 130
- [10] R.D. Ball and G. Ripka, The Regularization of the Fermion Determinant in Chiral Quark Models, (to be published in Procc. of the Conference on Many Body Physics, Coimbra, Portugal; September 20-25 1993), Saclay preprint SphT93/138
- [11] K. Kawarabayashi and M. Suzuki, Phys. Rev. Lett. **16** (1966) 255;
Riazuddin and Fayyazuddin, Phys. Rev. **147** (1966) 1071
- [12] K.M. Bitar and P.M. Vranas, A Study of the Nambu–Jona-Lasinio Model on the Lattice, FSU preprint FSU-SCRI-93-130
- [13] D. Espriu, E. de Rafael and J. Taron, Nucl. Phys. **B345** (1990) 22, Erratum ibid. **B355** (1991) 278
- [14] G. 't Hooft, Nucl. Phys. **B72** (1974) 461
- [15] E. Witten, Nucl. Phys. **B156** (1979) 269;
G. Veneziano, Nucl. Phys. **B159** (1979) 213;
P. Di Vecchia, Phys. Lett. **85B** (1979) 357
- [16] J. Gasser and H. Leutwyler, Ann. of Phys. **158** (1984) 142; Nucl. Phys. **B250** (1985) 465, 517, 539
- [17] M. Gell-Mann, R. Oakes and B. Renner, Phys. Rev. **175** (1968) 2195
- [18] S. Weinberg, Phys. Rev. Lett. **18** (1967) 507
- [19] E.G. Floratos, S. Narison and E. de Rafael, Nucl. Phys. **B155** (1979) 115
- [20] P. Pascual and E. de Rafael, Z. Phys. **C12** (1982) 127;
S. Narison, Z. Phys. **C14** (1982) 263
- [21] S. Narison, QCD Spectral Sum Rules, (World Scientific Lectures Notes in Physics - Vol. 26, Singapore 1990)
- [22] S.L. Adler, Phys. Rev. **177** (1969) 2426;
J.S. Bell and R. Jackiw, Nuovo Cim. **60** (1969) 47
- [23] W.A. Bardeen, Phys. Rev. **184** (1969) 1848
- [24] J. Wess and B. Zumino, Phys. Lett. **B37** (1971) 95;
E. Witten, Nucl. Phys. **B233** (1983) 422

- [25] Ll. Ametller et al., Nucl. Phys. **B228** (1983) 301;
A. Pich and J. Bernabéu, Z. Phys. **C22** (1984) 197
- [26] S.L. Adler and W.A. Bardeen, Phys. Rev. **182** (1969) 1517
- [27] M. Bando, T. Kugo and K. Yamawaki, Phys. Rep. **164** (1988) 217 and references therein
- [28] CELLO Colaboration, H.-J. Behrend et al., Z. Phys. **C49** (1991) 401
- [29] J. Bijnens, A. Bramon and F. Cornet, Z. Phys. **C46** (1990) 599;
J. Bijnens, Int. J. Mod. Phys. **A8** (1993) 3045
- [30] J. Prades, Massive Spin-1 Field Chiral Lagrangian from an Extended Nambu–Jona-Lasinio Model of QCD, Marseille preprint CPT-93/P.2871 (to be published in Z. Phys. C)
- [31] R.D. Ball, Phys. Rep. **182** (1989) 1

List of Figures

1	Plot of the dependence of the constituent quark mass M_i as a function of G_S for several values of m_i	4
2	The graphs contributing to the two point-functions in the large N_c limit. a) The class of all strings of constituent quark loops. The four-fermion vertices are either $\mathcal{L}_{\text{NJL}}^{\text{S,P}}$ or $\mathcal{L}_{\text{NJL}}^{\text{V,A}}$ in eq. (2.2) . The crosses at both ends are the insertion of the external sources. b) The one-loop case.	8
3	The inverse of the transverse vector two-point function for equal quark masses in the chiral limit, i.e. $\mathcal{M} \rightarrow 0$; for the ρ meson, i.e. $m_1 = m_2 = 3.2$ MeV and for the ϕ meson, i.e. $m_1 = m_2 = 83$ MeV. The units of q^2 are GeV^2	14
4	The transverse vector-two-point function for the chiral limit and for unequal quark masses, $m_1 = \bar{m}$ and $m_2 = m_s$. Note the kinematical pole at $q^2 = 0$. The units of q^2 are GeV^2	15
5	The running pseudoscalar mass squared, $m_{ij}^2(-q^2)$, as a function of q^2 for $m_i = m_j = 3.2$ MeV.	15
6	The graphs that need to be summed in the large N_c limit for the Vector-Pseudoscalar-Pseudoscalar three-point function. See text for explanation.	18
7	The graphs that need to be summed in the large N_c limit for the Pseudoscalar-Vector-Vector three-point function. See text for explanation.	22
8	The inverse of the vector form factor of the pion of eq. (5.8) . For the chiral limit and with all current quark masses equal to 3.2 MeV. Also plotted is the VMD approximation $M_V^2(-q^2)/(M_V^2(-q^2) - q^2)$ for the latter case.	27
9	The generalized KSRF relation. We plot $g_V(-q^2)$ for $g_A = 0.61$ (solid line); $g_A \rightarrow 1$ (short-dashed line) and $f_V(-q^2)/2$ (dashed line). The difference between the curves gives the violation of the KSRF relation. See text for further comments.	30
10	The inverse of the $\pi^0\gamma^*\gamma$ form factor for one photon on-shell and one off-shell as a function of the photon mass squared, q^2 . Notice the linearity in the Euclidean region. Plotted are the full result, $M_V^2(-q^2)/(M_V^2(-q^2) - q^2)$ (VMD-like) and the ENJL model without vector and axial-vector mesons ($g_A = 1$).	31